Mesoscale Self-Assembly of Hexagonal Plates Using Lateral Capillary Forces: Synthesis Using the "Capillary Bond"

Ned Bowden, Insung S. Choi, Bartosz A. Grzybowski, and George M. Whitesides*

Contribution from the Department of Chemistry and Chemical Biology, Harvard University, 12 Oxford Street, Cambridge, Massachusetts 02138

Received November 9, 1998. Revised Manuscript Received March 5, 1999

Abstract: This paper examines self-assembly in a quasi-two-dimensional, mesoscale system. The system studied here involves hexagonal plates ("hexagons") of poly(dimethylsiloxane) (PDMS; 5.4 mm in diameter, 0.9−2.0 mm thick), with faces functionalized to be hydrophilic or hydrophobic, floating at the interface between perfluorodecalin (PFD) and H_2O. The hexagons assemble by capillary forces originating in the interactions of the menisci at their hydrophobic and hydrophilic rectangular faces. The strength and directionality of the interactions can be tailored by manipulating the heights of the faces, the pattern of the hydrophobic faces, the pattern of hydrophobic regions *on* these faces, and the densities of the three interacting phases (organic liquid, aqueous liquid, polymeric solid). Examination of all 14 possible combinations of hydrophobic and hydrophilic faces on the hexagonal plates led to three outcomes: (i) the extension of the strategies of self-assembly from the molecular to the mesoscale, (ii) the demonstration of a system in which small objects can be designed to self-assemble into a variety of arrays, and (iii) the hypothesis that capillary forces between objects can, in some circumstances, be considered to form the basis for a "bond" between them—the capillary bond—and be used in synthesis in a way analogous to that in which noncovalent bonds are employed in molecular-scale synthesis.

Introduction

This paper extends the concepts underlying *molecular* self-assembly[1−6] to the self-assembly of macroscopic but small (that is, *mesoscopic*) objects.[7−10] Mesoscopic self-assembly (MESA) and molecular self-assembly share the characteristic that the forces between interacting components in an aggregate (capillary forces in our experiments in MESA; forces originating in noncovalent bonds for molecular self-assembly) are comparable to the forces that agitate them (shear forces due to stirring in MESA; intermolecular forces due to thermal, Brownian motion in molecular self-assembly). The formation of aggregates in both systems—whether of mesoscopic or molecular components—is therefore reversible at some level of agitation. Mesoscopic and molecular systems differ in their details: the nature and strength of the interactions, the character of the agitation that causes the components to encounter and separate from one another, and the statistics characterizing the distribution of energy among these components.

The word "mesoscopic" has two different but overlapping meanings. The first meaning is that common in physics: a mesoscopic object is one whose dimensions are comparable to the characteristic length of a phenomenon being examined.[10−12] Thus, in the study of electron mobility in a semiconductor, a mesoscopic object might be one with size comparable to the ballistic mean free path of an electron in that material (10−40 nm);[13] in optics, a mesoscopic object might be a diffraction grating, a structure with a periodicity having dimensions comparable to the wavelength of light (0.1−10 μm);[14,15] in cell biology, a mesoscopic object might be one with size similar to that of a cell (1−50 μm).[15−19] A second meaning of "meso" (that is, "middle") is that used by device fabricators: a size qualitatively intermediate between small (molecular) and large (easily manipulated by conventional means).[20] This loose meaning can include objects ranging in size from 10 nm to 1 mm, depending on the experiment and the system.

Although there are a range of techniques available for fabricating systems composed of mesoscopic components, few of these function by assembling *separate* small components.

(1) Desiraju, G. R. *Crystal Engineering: The Design of Organic Solids*; Elsevier: New York, 1989.

(2) Poirier, G. E. *Chem. Rev.* **1997**, *97*, 1117−1127.

(3) Bain, C. D.; Troughton, E. B.; Tao, Y.-T.; Evall, J.; Whitesides, G. M.; Nuzzo, R. G. *J. Am. Chem. Soc.* **1989**, *111*, 321−335.

(4) Lehn, J.-M. *Angew. Chem., Int. Ed. Engl.* **1988**, *27*, 89−112.

(5) Whitesides, G. M.; Mathias, J. P.; Seto, C. T. *Science* **1991**, *254*, 1312−1319.

(6) Whitesides, G. M.; Simanek, E. E.; Mathias, J. P.; Seto, C. T.; Chin, D. N.; Mammen, M.; Gordon, D. M. *Acc. Chem. Res.* **1995**, *28*, 37−44.

(7) Bowden, N.; Terfort, A.; Carbeck, J.; Whitesides, G. M. *Science* **1997**, *276*, 233−235.

(8) Terfort, A.; Bowden, N.; Whitesides, G. M. *Nature* **1997**, *386*, 162−164.

(9) Huck, W. T. S.; Tien, J.; Whitesides, G. M. *J. Am. Chem. Soc.* **1998**, *120*, 8267−8268.

(10) Terfort, A.; Whitesides, G. M. *Adv. Mater.* **1998**, *10*, 470−473.

(11) Rosen, A. *Adv. Quantum Chem.* **1998**, *30*, 235−272.

(12) Groma, I. *Phys. Rev. B: Condens. Matter* **1997**, *56*, 5807−5813.

(13) Kelly, M. J. *Low-Dimensional Semiconductors, Materials, Physics, Technology, Devices*; Oxford Science Publications, Clarendon Press: Oxford, 1995.

(14) Freeman, M. H. *Optics*, 10th ed.; Butterworth: London, 1990.

(15) Meyer-Arendt, J. R. *Introduction to Classical and Modern Optics*; Prentic-Hall, Inc.: Englewood Cliffs, New Jersey, 1995.

(16) Voet, D.; Voet, J. G. *Biochemistry*; John Wiley & Sons: New York, 1995.

(17) Singhvi, R.; Kumar, A.; Lopez, G. P.; Stephanopolous, G. N.; Wang, D. I. C.; Whitesides, G. M.; Ingber, D. E. *Science* **1994**, *264*, 696−698.

(18) Mrksich, M. *Curr. Opin. Colloid Interface Sci.* **1997**, *2*, 83−88.

(19) Chen, C. S.; Mrksich, M.; Huang, S.; Whitesides, G. M.; Ingber, D. E. *Science* **1997**, *276*, 1425−1428.

(20) Namba, S. *J. Phys. Soc. Jpn.* **1994**, *63*, 224−235.

The techniques most widely used for micro- and mesoscale fabrication[21]—photolithography, lift-off, e-beam writing, ion-beam writing, and reactive ion etching—generate planar patterns, rather than assemble components. In manipulation of individual components, the devices most commonly used include mechanical micromanipulators,[22,23] scanning probe devices,[24] and optical tweezers.[25,26] New techniques for assembling mesoscopic components would be welcome in microelectronics, microelectromechanical systems (MEMS), optoelectronics, and precision manufacturing of small systems.[21,27,28]

This paper describes the first phase of an effort to extend the principles of molecular self-assembly to mesoscale objects. The work has two direct inspirations: the formation of molecular crystals and life. Crystallization generates relatively simple, static structures characterized by long-range translational order; biology offers many examples of complex, dynamic systems comprising locally ordered components. There are many types of aggregates that illustrate different strategies for molecular self-assembly: examples include aggregates based on hydrogen bonds[29,30] and metal chelates,[31,32] self-assembled monolayers,[18,33] liquid crystals,[34,35] and arrays of oligonucleotides.[29−32] Molecular self-assembly is now guiding progress toward engineered molecular crystals.[36,37] Biology is replete with examples of molecular self-assembly at all levels of complexity: these include lipid bilayers, complex aggregates of proteins (e.g., the pyruvate decarboxylate complex, chaperones and proteosomes, and myosin filaments), and much more complicated structures (coated pits, gap junctions, viral capsids, double stranded DNA, and the ribosome).[16]

Mesoscale objects also self-assemble: examples include colloidal crystals,[38] bubble rafts,[39] two-dimensional arrays of nanometer- and micrometer-sized beads,[40,41] gold colloids assembled by DNA duplex formation,[42] sand piles,[43,44] and
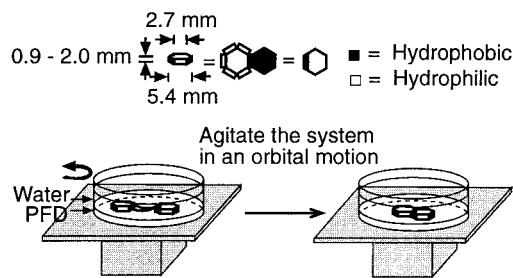
Figure 1. Schematic representation of two hexagonal plates (each having a hydrophobic bottom face, a hydrophilic top face, one hydrophobic side, and five hydrophilic sides) floating at the interface between PFD and water. The two plates are pulled together by capillarity, that is, by minimization of the area of the PFD/H₂O interface.

grains of sand sliding in a rotating cylinder.[45,46] While these arrays demonstrate mesoscale aggregation or structure in a system of small particles, these particles all have approximately spherical or circular symmetry, give close-packed arrays, and are, as a result, not appropriate as models for studying the assembly of complex structures from components with lower symmetries.

We wished to develop systems that would give us a substantial choice both in the shape of the components and the form of the forces and potential functions through which they interacted. Here we describe one system that is proving both convenient experimentally and rewarding conceptually. This system consists of small (5.4 mm across, 0.9−2 mm high), hexagonal plates of poly(dimethylsiloxane) (PDMS; $\rho = 1.05$ g/cm³),[47] whose faces have been differentiated into hydrophilic and hydrophobic surfaces, floating at the interface between water ($\rho = 1.00$ g/cm³ at 20 °C) and a dense nonpolar liquid (perfluorodecalin, PFD; $\rho = 1.91$ g/cm³), and interacting through the menisci formed at these faces, that is, through capillarity (Figure 1).[41,48,49] We have briefly described experiments demonstrating the ability of this and related systems to form ordered aggregates.[7] Here we characterize this system and set the stage for further studies of more complex systems. Specifically, in this work we have characterized the aggregates that assemble from each of the 14 different hexagons that can be formed by permuting hydrophobic and hydrophilic surfaces on the six rectangular faces of the hexagonal plates (Figure 2); in all of these hexagons, one of the two large hexagonal faces (the bottom face) was hydrophobic, and the second, upper face was hydrophilic. For all of these hexagons, the hydrophobic surfaces were unmodified PDMS (-OSiMe₂-; $\theta_a^{H_2O} = 108°$);[50] the hydrophilic surfaces were PDMS that had been oxidized in an oxygen plasma and had formed a thin, hydrated silicate layer (-SiO₂·nH₂O, $\theta_a^{H_2O} = 30°$).[51,52]

Nomenclature. Symmetries of the Patterns. In the diagrams, we represent the hydrophobic and hydrophilic faces as thick and thin lines, respectively, along the edges of a top view of the hexagons (Figure 2). We describe the pattern of the hydrophobic faces of the hexagons by labeling these faces as

(21) Madou, M. *Fundamental of Microfabrication*; CRC Press: New York, 1997.

(22) Konig, K. *SPIE-Int. Soc. Opt. Eng.* **1998**, 178−182.

(23) Walz, J. Y. *Curr. Opin. Colloid Interface Sci.* **1997**, *2*, 600−606.

(24) Wiesendanger, R. *Proc. Natl. Acad. Sci. U.S.A.* **1997**, *94*, 12749−12750.

(25) Berry, R. M.; Berg, H. C. *Proc. Natl. Acad. Sci. U.S.A.* **1997**, *94*, 14433−14437.

(26) Shivashankar, G. V.; Libchaber, A. *Appl. Phys. Lett.* **1997**, *71*, 3727−3729.

(27) Nagler, O.; Trost, M.; Hillerich, B.; Kozlowski, F. *Sens. Actuators, A* **1998**, *A66*, 15−20.

(28) Godehardt, R.; Heydenreich, J.; Popescu-Pogrion, N.; Tirnovan, M. *Thin Solid Films* **1998**, *317*, 235−236.

(29) Philip, D.; Stoddart, J. F. *Angew. Chem., Int. Ed. Engl.* **1996**, *35*, 1154−1196.

(30) Rebek, J., Jr. *J. Chem. Soc. Rev.* **1996**, *96*, 255−263.

(31) Saalfrank, R. W.; Bernt, I.; Uller, E.; Hampel, F. *Angew. Chem., Int. Ed. Engl.* **1997**, *36*, 2482−2485.

(32) Stang, P. J.; Olenyuk, B.; Fan, J.; Arif, A. M. *Organometallics* **1996**, *15*, 904−908.

(33) Whitesides, G. M.; Laibinis, P. E. *Langmuir* **1990**, *6*, 87−96.

(34) Trzaska, S. T.; Swager, T. M. *Chem. Mater.* **1998**, *10*, 438−443.

(35) Knawby, D. M.; Swager, T. M. *Chem. Mater.* **1997**, *9*, 535−538.

(36) Reddy, D. S.; Panneerselvan, K.; Pilati, T.; Desiraju, G. R. *J. Chem. Soc., Chem. Commun.* **1993**, 661−662.

(37) Schwiebert, K. E.; Chin, D. N.; MacDonald, J. C.; Whitesides, G. M. *J. Am. Chem. Soc.* **1996**, *118*, 4018−4029.

(38) Murray, C. B.; Kagan, C. R.; Bawendi, M. G. *Science* **1995**, *270*, 1335−1338.

(39) Schober, S. T.; Friedrich, J.; Altmann, A. *J. Appl. Phys.* **1992**, *71*, 2206−2210.

(40) Kralchevsky, P. A.; Nagayama, K. *Langmuir* **1994**, *10*, 23−36.

(41) Yamaki, M.; Higo, J.; Nagayama, K. *Langmuir* **1995**, *11*, 2975−2978.

(42) Elghanian, R.; Storhoff, J. J.; Mucic, R. C.; Letsinger, R. L.; Mirkin, C. A. *Science* **1997**, *277*, 1078−1080.

(43) Jaeger, H. M.; Nagel, S. R. *Science* **1992**, *255*, 1523−1531.

(44) Makse, H. A.; Havlin, S.; King, P. R.; Stanley, H. E. *Nature* **1997**, *386*, 379−382.

(45) Zik, O.; Levine, D.; Shtrikman, S. G.; Stavans, J. *Phys. Rev. Lett.* **1994**, *73*, 644−647.

(46) Knight, J. B.; Jaeger, H. M.; Nagel, S. R. *Phys. Rev. Lett.* **1993**, *70*, 3728−3731.

(47) Publication No. 10-177-87, Dow Corning, Midland, MI.

(48) Fortes, M. A. *Can. J. Chem.* **1982**, *60*, 2889−2895.

(49) Davis, H. T. *Statistical Mechanics of Phases, Interfaces, and Thin Films: Advances in Interfacial Engineering*; VCH: New York, 1996.

(50) Owen, M. J. *J. Coatings Technol.* **1981**, *53*, 49−53.

(51) Morra, M.; Occiello, E.; Marola, R.; Garbassi, F.; Humphrey, P.; Johnson, D. *J. Colloid Interface Sci.* **1990**, *137*, 11−24.

(52) Fakes, D. W.; Davies, M. C.; Browns, A.; Newton, J. M. *Surf. Interface Anal.* **1988**, *13*, 233.
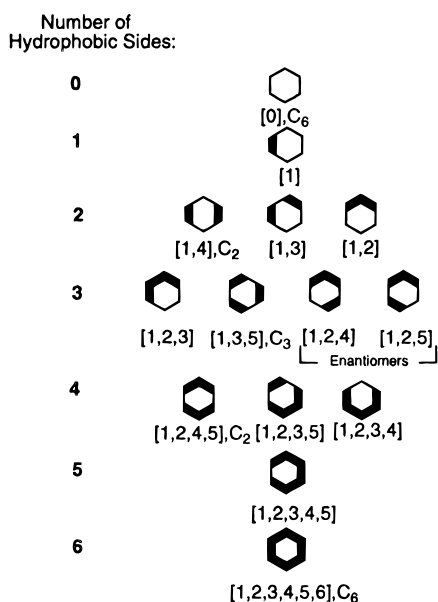
Figure 2. The fourteen different hexagons that can be constructed from all possible combinations of hydrophobic and hydrophilic faces on a hexagonal plate. Dark lines indicate hydrophobic faces, thin lines indicate hydrophilic faces. Numbers refer to the hydrophobic faces. Hexagons with a C_n (n > 1) axis perpendicular to the large hexagonal faces are labeled. All of the hexagons except the chiral ones ([1,2,4] and [1,2,5] hexagons) have one or more mirror planes of symmetry. In each the top face is hydrophilic and the bottom hydrophobic.

numbers in square parenthesis as [*x,y,z*...], where *x*, *y*, *z*... refer to the hydrophobic faces. For example, a [1,2] hexagon is one with two adjacent hydrophobic faces, and the other four faces are hydrophilic. The numbering begins with a hydrophobic face and continues by numbering the faces of the hexagons from above in a clockwise direction. For unsymmetrically patterned hexagons, the numbering starts at the face that has the longest set of adjacent hydrophobic faces (e.g., [1,2,4] rather than [1,4,5]). The [0] hexagon has only hydrophilic faces. In the text, the hydrophobic faces will be in square parenthesis; the hydrophilic faces will not be in parenthesis. For example, in discussing [1,2] hexagons we will refer to the hydrophobic faces as the [1] and [2] faces and the hydrophilic faces as the 3, 4, 5, and 6 faces.

In a few experiments, we used hexagons in which individual faces were divided into hydrophilic and hydrophobic regions. Faces of the hexagons that are part hydrophobic and part hydrophilic are labeled by placing in a subscript the areas along the face that are hydrophilic and hydrophobic (indicated by the number being underlined). A face where the middle one-half is hydrophobic and the edges are hydrophilic would be represented by $x_{1:\underline{2}:1}$; the *x* refers to the number of the face and the numbers in subscripts refer to the hydrophilic and hydrophobic areas along the face. Thus, a [$1_{1:\underline{2}:1}, 2_{1:\underline{2}:1}$] hexagon has two adjacent faces that are one-half hydrophobic. In all of the systems of this type examined in this paper, the middle one-half of the area of a face is hydrophobic, and the edges are hydrophilic.

Figure 2 identifies the systems that have C_2, C_3, and C_6 symmetries. The distinction between hexagons having a center of symmetry and those that do not is important: the vertical components of the capillary forces on hexagons that have a centrosymmetric pattern of hydrophobic faces are balanced, and these hexagons are orientated with the hexagonal faces parallel to the mean plane of the PFD/H$_2$O interface; for the others, the balance of forces is unsymmetrical, and each floats with a more-or-less pronounced tilt relative to the interface (Figure 3a).
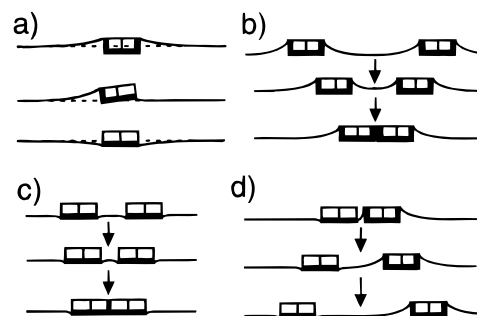
Figure 3. (a) Hexagons are pulled into the interface by the capillary forces on the hydrophobic faces. Dashed lines indicate the level of the PFD/H$_2$O interface far from the objects. Hexagons where these forces are balanced float evenly at the interface; hexagons with an unbalanced distribution of forces are tilted at the interface. (b), (c), and (d) Three types of capillary interactions between hydrophobic and hydrophilic objects at the PFD/H$_2$O interface. In (b) the PFD wets the hydrophobic faces and forms positive menisci. When two faces come together, the net area of the PFD/H$_2$O interface decreases. This decrease is energetically favorable, brings the pieces together, and holds them in close proximity. In (c) the objects are hydrophilic and sink slightly into the PFD/H$_2$O interface; this sinking creates a small negative meniscus. When these objects approach one another, the area of the PFD/H$_2$O interface again decreases, but the decrease is small compared to the decrease in (b). In (d) a hydrophobic face—with a positive meniscus—is repelled by a hydrophilic face with a negative meniscus. When these objects move toward one another, the area of the PFD/H$_2$O interface *increases*. Thick lines and thin lines indicate hydrophobic and hydrophilic faces, respectively.

The menisci on the hydrophobic faces are formed when PFD wets these faces; we will call these "positive" menisci (*menisci rising above the mean plane of the interface*; Figure 3b). The menisci on the hydrophilic faces are formed when H$_2$O wets these faces; we will call these "negative" menisci (*menisci sinking below the mean plane of the interface*; Figure 3c).

To show the height of the menisci along the hydrophobic faces on the hexagons that are tilted at the interface, we draw top and side views of the hexagons. In the top view we indicate the size of the positive menisci with a "+" symbol; the larger the "+" symbol, the larger the meniscus is at that part of the face.

The [1,2,4] and [1,2,5] hexagons are chiral. Although we exploit this chirality in only a limited way, it is important in other problems in recognition and aggregation involving these hexagons and in more complex structures derived from them.

In some optical micrographs, we draw both the top and the side views of the hexagons. We use this representation when we wish to show the relative thicknesses of the hexagons. The side views are drawn to scale for each hexagon.

Design of the System

PDMS. We chose PDMS for three reasons. (i) It is easily fabricated into the required shapes. (ii) Its unmodified surface is hydrophobic but can easily be made hydrophilic by oxidation in an oxygen plasma. We have developed several methods for protecting faces of the PDMS from oxidation by the plasma, so that we can selectively pattern the faces of the objects to be hydrophobic or hydrophilic. (iii) The bulk PDMS is easily modified. We can dye selected parts or all of the PDMS; we can add materials with useful properties (electrical, magnetic, or optical) or denser materials with useful properties (such as iron oxide) to the PDMS to change its density or other properties.

Shapes and Dimensions. We chose to fabricate hexagons because hexagons offered a reasonable number of different patterns of hydrophobic and hydrophilic faces; hexagons can also be assembled into large, ordered arrays. We used hexagonal PDMS plates having the dimensions shown in Figure 1; the thickness of the plates was usually between 1.0 and 1.3 mm, although thicker plates were also easily generated and were occasionally used. The thickness of the plates was usually chosen to be as thin as could be easily fabricated, to minimize the attractive forces between the hexagons so that the assembly could be reversible. Using plates of this thickness also minimized the type of irreversible interaction between hexagons that occurred when two hydrophobic faces came into contact with no intervening PFD.[53] We therefore chose the thicknesses of the hexagons so that the PFD would wet the hydrophobic faces completely and thus preserve the reversibility of assembly of the objects. The hexagons could be reliably and reproducibly fabricated with thicknesses as small as 0.9 mm; the softness of the PDMS made fabricating thinner hexagons with well-shaped faces impractical.

The size of the hexagons (5.4 mm in diameter) was chosen for four reasons. (i) Hexagons of this size were easy to fabricate. (ii) Experimental observation of hexagons was convenient; both individual hexagons and aggregates could easily be observed by eye and recorded using optical microscopy. (iii) Hexagons of this diameter were small enough that a statistically significant number of them (50−100) could be studied in a small dish. (iv) The dimensions of the particle were of the same order of size as those of the capillary interactions and menisci through which they interact.

The Fluid/Fluid Interface: PFD/H_2O. We selected the PFD/H_2O pair because it had four useful characteristics.[54] (i) It had a high liquid/liquid interfacial free energy ($\gamma = 0.05$ J m^{-2} = 50 erg cm^{-2}) and hence high capillary forces.[55,56] (ii) Neither liquid swelled PDMS. (iii) The densities of the two liquids bracketed that of PDMS. (iv) A thin, lubricating layer of PFD separated the faces on two hexagons even when they were "in contact": that is, at closest approach. The system was simplest if the PDMS hexagons had a density close to that of water, since this configuration simplified analysis of the capillary interactions.

We chose to use a liquid/liquid interface instead of an air/liquid interface as the plane in which self-assembly occurred because the assemblies were more reproducible at the former. Objects at the air/water interface did not float reliably; they were easily pinned at the interface at various angles. Objects at the PFD/H_2O interface floated at reproducible angles relative to the interface. The liquid/liquid interface also gave us many opportunities to tailor the forces between the objects. In this paper, for example, we have increased the density of the water by adding KBr and increased the density of the PDMS by curing iron oxide into it.[57]

(53) Two hydrophobic PDMS faces that come into contact in water without PFD present stick irreversibly.

(54) We added perfluoromethyldecalin to the perfluorodecalin. The two liquids had similar densities, boiling points, and surface tensions; thus, we continued to label the mixture of solvent perfluorodecalin because PFD was the major component.

(55) Markina, Z. N.; Bovkun, O. P.; Zadymova, N. M.; Roskete, E.; Shchukin, E. D.; Makarov, K. N.; Gervits, L. L. *Zh. Vses. Khim. O-va. im. D. I. Mendeleeva* **1988**, *33*, 346−348.

(56) The units for interfacial free energy can be expressed as work per unit area (J m^{-2} or erg cm^{-2}) or as force per unit length (N m^{-1} or dyne cm^{-1}).

(57) Other opportunities exist to tailor the forces and potential functions at the liquid/liquid interface; we will describe these opportunities in future papers.

**Table 1.** Tilt Angles, α, for the 1.2-mm and 2.0-mm Thick Hexagons

Hexagon	α ($^{\circ}$)[a] 1.2 mm	2.0 mm
⬡	7 ± 2	
⬡	3 ± 1	
⬡	14 ± 1	26 ± 2
⬡	3 ± 2	
⬡	6 ± 2	
⬡	15 ± 1	30 ± 1
⬡	5 ± 2	
⬡	14 ± 1	
⬡	9 ± 2	
⬡⬡	6 ± 1[b]	

[a] The uncertainities were standard deviations of at least 25 measurements on different hexagons. [b] In this entry the two hexagons were self-assembled as a dimer with the hydrophilic faces in contact; the hexagons in the dimer were tilted in the same direction as the monomeric [1,2,3,4,5] hexagons.

Differential Wetting and Capillary Forces. The hexagons float at the PFD/H_2O interface, and menisci of PFD wet the hydrophobic faces. When two hydrophobic faces of the hexagons come into contact or close proximity, these menisci are eliminated. Elimination of the menisci reduces the area of the PFD/H_2O interface, lowers the free energy of the system, and holds the objects together. Under the influence of capillary forces, the hydrophobic faces are attractive over long distances; for hexagons of the geometry used here (Figure 1), the hexagons move toward one another when they are separated by distances comparable to 3 times their heights (that is, approximately the length of a face).

In a system comprising hexagons of PDMS ($\rho = 1.05$ g/cm^3), water ($\rho = 1.00$ g/cm^3), and PFD ($\rho = 1.91$ g/cm^3), the hexagons floated at, rather than sank completely into, the interface. Although the hydrophilic faces show a slight negative meniscus and interact slightly attractively, the dominating interactions for all of the hexagons except the [1,2,3,4,5] hexagons are those involving the positive menisci. In general, two faces with positive menisci are strongly attractive, two faces with negative menisci are weakly attractive, and a face with a positive meniscus is repelled by a face with a negative meniscus (Figure 3).

Orientation of the Hexagons at the Interface: Tilting and Sinking. The capillary forces on the hexagons are sufficiently strong to cause hexagons with an unsymmetric pattern of hydrophobic faces to tilt relative to the plane of the PFD/H_2O interface, and hexagons with a symmetric pattern of hydrophobic faces to be pulled more deeply into the interface, than would be predicted by the densities of the PDMS, PFD, and H_2O. Because the tilt of the hexagons had important consequences for the assemblies, we measured the angles of tilt for several hexagons (Table 1), and we estimated the extent to which symmetrically substituted hexagons were pulled into the interface (Table 2). Details of the measurements and calculations
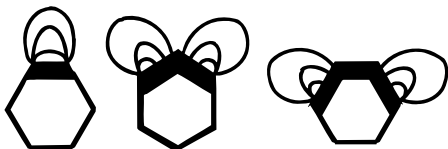
Figure 4. Contours of the positive menisci along the hydrophobic faces of the [1], [1,2], and [1,2,3] hexagons are represented by the lines. These lines represent topographical estimates (by eye) of the shapes of the menisci.

Table 2. Calculated Distance That the 1.2-mm Thick Hexagons Sink into the PFD/H$_2$O Interface under the Influence of Bouyant, Gravitational, and Capillary Forces

hexagon	distance sunk into the interface (mm)
[0]	0.01
[1,4]	0.33
[1,3,5]	0.49
[1,2,4,5]	0.65
[1,2,3,4,5,6]	0.97

are given in the Supporting Information and in the section dealing with capillary forces.

The extent of the tilt is affected by the geometry of the hexagons and the pattern of the hydrophobic faces. Some hexagons ([1,2], [1,2,3], [1,2,3,4], and [1,2,3,4,5] hexagons) are so strongly tilted that one or more hydrophobic faces or vertexes is essentially buried in the PFD/H$_2$O interface. These faces and vertexes have only small positive menisci associated with them and are only weakly attracted to one another. The hydrophilic face opposite the buried hydrophobic face can be pulled *above* the interface and generate a small, positive meniscus (Figure 3a).

Self-Assembly Matches the Contours of the Menisci. The contours of the menisci are an important factor in the self-assembly of the hexagons; the hexagons self-assemble to overlap the contours of the menisci on the two interacting faces. When we describe the contours of the menisci, we are referring to their heights, relative to the mean plane of the interface, along the sides of the hexagons and extending out across the interface (Figure 4).

Hexagons with a symmetric pattern of hydrophobic faces have menisci with very different contours than do hexagons with an unsymmetric pattern. Because symmetrically patterned hexagons float approximately parallel to the interface, the contours of the menisci are symmetrical about the center of each face. These hexagons assemble to match the contours of their menisci by assembling with their faces opposed to one another. Because unsymmetrically patterned hexagons float at an angle relative to the interface, the contours of the menisci are unsymmetrical about the center of each tilted face, that is, the menisci are higher at one end of the face than at the other end. These hexagons assemble so as to match the contours of their menisci, that is, the tallest part of the menisci on two interacting faces are opposed.

Lateral Motion. Capillary forces bring hexagons into contact rapidly once random encounters at the agitated PFD/H$_2$O interface bring hydrophobic faces on separate hexagons to within a few mm. Tests at an unstirred interface establish that it takes approximately 2 s for two hexagons to collapse into a dimer over a distance of 5 mm. We have not studied the dynamics of these events sin detail, but qualitatively, as the hexagons move toward one another, they begin to align their hydrophobic faces. Once "in contact" (that is, at the closest separation but still separated by a thin PFD layer—much less than 1 mm) the

hexagons move laterally relative to one another. We believe that the thin lubricating layer of PFD is essential to forming organized aggregates: it allows the hexagons to adjust their positions to oppose the hydrophobic faces and also allows them to separate. Lateral motion is required for the objects to find the lowest energy configuration of the two contacting faces.

There are two pieces of evidence for this layer of PFD. First, in some but not all cases it is visible by inspection; the hexagons do not quite touch (see, for example, Figure 8c). Second, if two hydrophobic faces of PDMS come into contact in water without PFD present, they stick irreversibly.

Experimental Methods

Fabrication and Dyeing of the Hexagons. We will give a brief description of the fabrication and dyeing of the hexagons; the full details can be found in the Supporting Information.

The hexagons were made by curing PDMS in a hexagonal mold. The hexagons were removed from the mold and dyed red, blue, or a combination of red and blue. In many cases we dyed the hexagons two colors to identify the hydrophobic faces; the hexagons with two colors were fabricated by first dyeing the hexagons red and then dyeing certain faces blue. The blue dye (crystal violet) was soaked into the PDMS with methylene chloride, when the hexagons were dried, the blue dye did not diffuse further in the PDMS. Therefore, we were able to dye selected faces blue.

Selected faces of the hexagons were covered with Scotch tape prior to oxidation. The oxidation of the PDMS in the plasma cleaner formed a surface terminated in SiOSi and SiOH groups.[51] The oxidized surfaces were hydrophilic ($\theta_a^{H_2O} = 30°$); the faces covered with tape remained hydrophobic. After the oxidation, the tape was removed, and the pieces were cut at both ends to generate two hexagons with new, hexagonal hydrophobic faces. The tops (in contact with the water) of the hexagons were hydrophilic and the bottoms (in contact with the PFD) were hydrophobic. Hexagons with partially hydrophobic faces were fabricated by cutting a length of Scotch tape 1.3-mm wide and using this tape to cover the face of the hexagonal objects prior to the oxidation. We placed the newly cut hydrophobic face in contact with the PFD/H$_2$O interface with tweezers to ensure their correct orientation. Oxidized PDMS exposed to air becomes hydrophobic within 24 h; oxidized PDMS kept at the PFD/H$_2$O interface remained hydrophilic for much longer than a week.

For each experiment the hexagons were cut to the same thickness, to the best of our abilities. After each experiment was complete, we measured the average thickness of the hexagons by placing them in stacks of 10–20 and measuring the thickness of the stack.

Interconversion Among Monomers and Aggregates: Steady State. All self-assembling systems require interconversion among different states—unaggregated, incorrectly aggregated, and ordered—for the system to form large ordered aggregates. In molecular self-assembly, thermal energy agitates the molecules and causes equilibration; the distribution of thermal energies is described by the Boltzmann equation. In the experiments described here, the system is less well defined in terms of the activation of the plates since the agitation is nonuniform across the dish. The suspension of hexagons at the PFD/H$_2$O interface was agitated by using an orbital shaker. The dish moved with a circular motion in the resting plane of the PFD/H$_2$O interface, and the hexagonal plates were agitated by the resulting swirling motion. The plates aggregated in the vortex in the center of the dish and spun in an irregular motion around this center. After a time (typically less than 60 min at a frequency of rotation, ω (s^{-1}), for the orbital shaker of $\omega = 1.5$ s^{-1}) the objects would approach a steady state, with some distribution of structures. The *types* of structures present in the arrays were reproducible from experiment to experiment; the *sizes* of the arrays (for example, exactly how many hexagons were present in the lines formed from [1,4] hexagons) were not.

The rate of interconversion among the arrays was controlled by the strength of the interaction between the hexagons and by the intensity of agitation supplied to the system. To minimize the attractive capillary

interactions between the hexagons, we made them as thin as we practically could (1.0−1.3 mm).

At orbital frequencies of $\omega = 1.5$ s^{-1}, two [1] hexagons, 1.1-mm thick and held together by one set of hydrophobic faces, dissociated with a rate of $\sim 5 \times 10^{-5}$ sec^{-1} or ~ 0.2 h^{-1} (rates of association depended on the concentration of hexagons on the surface).[58] This rate is slow relative to that of larger aggregates, and we believe that the rate of dissociation is strongly influenced by the shear experienced by the aggregate. The shear across the dimer induced by the motion of the fluids is small compared with the shear across larger arrays, and larger arrays readily break into smaller arrays at high rates of agitation. Small arrays of hexagons held together by many hydrophobic/hydrophobic interactions were often stable and did not dissociate even at the highest rate of agitation ($\omega = 1.5$ s^{-1}). For large arrays, disaggregation by shear competed with aggregation by capillary forces. Often several smaller arrays formed at high rates of agitation and then coalesced into one large array when the intensity of agitation was decreased.

Visualizing Menisci and Tilting at the PFD/H$_2$O Interface. We identified menisci as positive or negative, and established the orientation of the tilts of the hexagons, by observing them in the plane of the interface from the side of the dish. To characterize the menisci and tilting more quantitatively, we used two procedures: (i) we took optical micrographs of single hexagons at the interface and estimated the tilt from the photographs, (ii) we used an optical technique (described in the Supporting Information) by means of light reflected from their tops that quantified their tilt. For several hexagons ([1], [1,4], 1.2-mm and 2.0-mm thick [1,2], 1.2-mm and 2.0-mm thick [1,2,3], [1,2,3,4], and [1,2,3,4,5] hexagons), we also took optical micrographs of the hexagons from the side after they had self-assembled into arrays: qualitatively, the hexagons remained tilted in the same direction relative to the pattern of hydrophobic faces before and after assembly. In general, we have not quantified the tilt of the hexagons in the arrays.

To measure the tilt angles of the hexagons quantitatively using reflection of light, we fabricated hexagons with a small gold mirror on the top, and we used a procedure that made the top and bottom faces parallel. The details of the measurements are given in the Supporting Information. The tilt angles reported in Table 1 were the average of over 25 measurements of different hexagons; these angles were in agreement with estimates taken by observation from the side.

Metastable and Unstable Aggregates: Assembly of Arrays by Hand. Because this system used millimeter-sized hexagons that could be manipulated by hand, we had the useful option to assemble arrays that we believed were relatively unstable. We used this method when we wanted to characterize the stability of aggregates either that we did *not* observe as products of aggregation of a particular type of hexagon (see, for example, the section on the [1,2] hexagons), but that seemed plausible, or that we did observe as minor products of aggregation of a particular type of hexagon (see, for example, the section on the [1,3] hexagons) and we wished to test for stability. By preparing these aggregates independently and examining their stabilities under agitation, we could infer if the absence of a particular aggregate in an experiment reflected low stability or a slow rate of formation (see the section on the [1,2,4,5] hexagons) and thereby infer whether the arrays that formed were an artifact of the starting conditions or reflected the characteristics of the hexagons (see the section on [1,3] hexagons).

In examining metastable aggregates, we assembled the hexagons by placing them in the correct orientation at the interface with tweezers. We identified the hydrophobic faces by noting the curvature of the menisci at the PFD/H$_2$O interface or by coloring the hexagons in a way that distinguished the hydrophobic and hydrophilic faces from one another. After assembling an array, we checked that the hexagons were correctly orientated by agitating at $\omega = 0.5$ s^{-1}. This rate of agitation would break apart two weakly interacting hydrophilic faces but leave

together arrays assembled by opposition of hydrophobic faces. When we were satisfied that the hexagons were orientated correctly, we increased the intensity of agitation by increasing ω.

Procedure for Self-Assembly. Agitation. We took the PFD from the bottom of a separatory funnel containing PFD and water, and did not use PFD close to the interface: this procedure excluded particles floating at the interface. Deionized water was poured onto the PFD. A typical experiment used a dish 14.5 cm in diameter containing 150 mL of PFD, 250 mL of H$_2$O, and 80 hexagons. Before agitation, all of the air bubbles were removed from the PFD/H$_2$O interface; air bubbles had menisci that interacted with the hexagons and disrupted the arrays.[59]

With the use of tweezers hexagons were placed at the PFD interface in the orientation with the hydrophobic hexagonal face down. The hexagons were agitated with an orbital shaker in a circular motion— counterclockwise when viewed from the top of the assembly[60]—with a diameter of approximately 2.5 cm (Figure 1) at frequencies from $\omega = 0.5$ to 1.5 s^{-1}.

We tested the ability of PFD to wet the hydrophobic faces by pushing into the PFD/H$_2$O interface long, unoxidized hexagonal rods of PDMS that were clear, blue, red, and a combination of blue and red. As the rods were pushed into the interface, the PFD slightly wet the rods that were either clear or blue, and small, positive menisci formed. These positive menisci were much smaller than those that formed when the rods were pulled out of the interface. The difference in the size of the menisci can be attributed, in part, to the variation in the advancing and receding contact angles of PFD on the clear and blue PDMS (Table 3). The PFD did not spontaneously wet the rods that were colored red or a combination of red and blue; as these rods were pushed into the interface, negative menisci formed. The PFD formed large, positive menisci when the hexagons were pulled out of the interface. In the experiments described in this paper we initially pushed the hexagons into the interface or agitated them with the orbital shaker for approximately 30 min to ensure that that PFD wet all of the hydrophobic faces, including those faces dyed red. The menisci were stable once formed on the faces.

At the beginning of each experiment, we separated most of the interacting hexagons manually by pushing them apart with the tip of a glass pipet. We agitated the system at rotational frequencies up to $\omega = 1.5$ s^{-1}; above this rate, droplets of PFD formed and rested at the interface.[61] Although assemblies were typically conducted entirely at $\omega = 1.5$ s^{-1}, some arrays were allowed to form at a lower rates of agitation, or the assembly was agitated at $\omega = 1.5$ s^{-1} for a period of time, and the intensity of agitation was then decreased by lowering ω to $0.5-1.0$ s^{-1}. In experiments in which this annealing process produced the best (largest, most ordered) aggregates, the hexagons assembled into small arrays at the higher rate of agitation and then condensed into larger arrays at the lower rate of agitation. We will describe the method of agitation used in any experiment not conducted entirely at $\omega = 1.5$ s^{-1}. After the assembly was stopped, the system was carefully placed on a light box and photographed.

When the agitation was weakened or stopped, the isolated arrays joined by strong capillary interactions between hydrophobic faces tended to condense further due to interactions between the weakly interacting hydrophilic faces and between any hydrophobic faces that remained exposed. Some of the aggregates that formed as the agitation was weakened were ordered (see the sections on [1,2] and [1,2,3,4] hexagons), but others showed no order when the agitation was weakened or stopped. Most of the figures that follow show optical micrographs of the arrays as they existed when the agitation had stopped. For the [1$_{1:2:1}$, 2$_{1:2:1}$], [1,2,4], and [1,2,5] hexagons, we also carefully separated the aggregates at the weak junctions, so that only the hexagons that had been in contact with one another during the agitation were in contact in the photographs. This separation gives the reader an accurate

(58) The dissociation rate was measured by observing the dissociation of 23 dimers of [1] hexagons agitated at $\omega = 1.5$ s^{-1}. The 23 pairs self-assembled through the interaction on the [1] faces. We observed the hexagons for 1.5 h and counted the number of dimers that dissociated. The dissociated hexagons readily reassembled into dimers, usually within 5 min after the dimer had fallen apart. The process was repeated twice. In the 4.5 h of observing the dimers, 21 pairs of hexagons dissociated.

(59) There were several sources for the air bubbles, including the air trapped along the sides of the dish and air bubbles brought to the interface with the hexagons.

(60) The motion of the hexagons at the interface was chiral. We did not exploit this chirality, but it is important to note for other systems.

(61) At high rates of agitation ($\omega > 1.5$ s^{-1}) the interface became turbid. Bubbles of PFD formed at the interface; these bubbles disrupted the capillary interactions between the PDMS hexagons.

assessment of the forms of the arrays that were stable *during the agitation*. We include pictures taken before (Figures 7a and 8a) and after (Figures 7b and 8b) separating the [1] and [1,4] hexagons by hand as examples of arrays that were stable during agitation and the more condensed aggregates that formed after the agitation had been stopped.

After the picture was taken, we would examine the orientations of the hexagons in the arrays. We used two strategies to establish this orientation. The first relied on inferring the pattern of hydrophobic and hydrophilic faces by observing the menisci; the second combined fabrication with dyeing, so that hydrophobic and hydrophilic faces were color coded (see the Supporting Information). The two methods were generally equally reliable, but the method based on dyeing gave more information in complex aggregation (e.g., the [1,2,3,4,5] hexagons in Figure 18) and also produced information that was readily interpreted from optical micrographs. In general, we used the first method for exploratory studies and the second, less convenient but more informative procedure, to document final results.

After each experiment, most of the hexagons were pushed apart with a glass pipet and the experiment was repeated. Each system was allowed to assemble a minimum of five times (and often many times more); the figures reflect the arrays that formed during each of these cycles.

Forty-eight hours after the hexagons were oxidized, we discarded them. If the hexagons were used for longer times, the assembly became slower and less reliable. We believe this degradation in capacity to self-assemble was due to the leaching of organic compounds from the PDMS and dye into the PFD/H_2O interface.

Results and Discussion

Characterization of Aggregates Formed From Hexagons With Different Patterns of Hydrophobic and Hydrophilic Faces. [0] Hexagons. These hexagons have no hydrophobic faces. We initially predicted that they would be only weakly attracted by capillary forces. Since PDMS ($\rho = 1.05$ g/cm^3) is slightly more dense than water ($\rho = 1.00$ g/cm^3), the hexagons sink slightly into the PFD, and the small negative menisci that form attract the hexagons weakly to one another. To demonstrate that the tendency of the [0] hexagons to assemble into arrays depended on the sense and size of the menisci, we carried out two sets of experiments (Figure 5). In one, we increased the depth of the negative meniscus by increasing the density of the PDMS hexagons relative to water by curing iron oxide into them. In the second, we eliminated the meniscus entirely, and even formed small, positive menisci, by increasing the density of the water relative to PDMS by adding KBr.
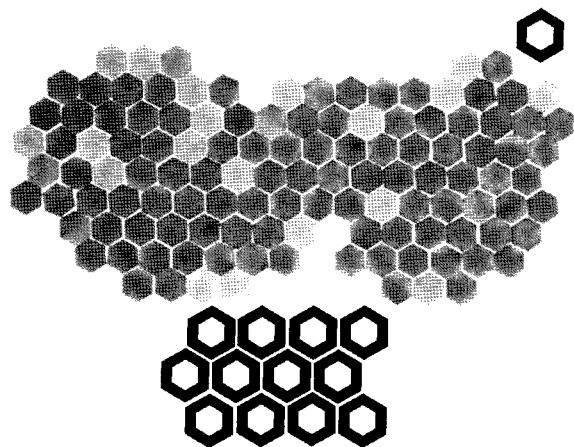
Increasing the Depth of the Negative Meniscus. The hexagons containing iron oxide (Figure 5a) had density of 1.33 g/cm^3; the density of water was 1.00 g/cm^3. The hexagons sank into the PFD/H_2O interface; the resulting capillary forces between the negative menisci were strong enough to form an ordered array even under mild agitation ($\omega = 0.75$ s^{-1}).

Eliminating and Inverting the Negative Meniscus. The success of these experiments depended on using hexagons whose bottoms were as flat as possible. Hexagons produced by the normal method were unsatisfactory: the step that generated the hydrophobic hexagonal bottom face involved cutting oxidized "prehexagons" with a razor blade. This mechanical cut left the bottom—and the junction of the bottom with the side faces— slightly rough (the roughness was in the form of an uneven surface where the thickness of the hexagon varied by several hundred micrometers); this roughness, in turn, generated micromenisci even when the water was adjusted to be isodense with the PDMS. The rough-bottomed hexagons interacted sufficiently strongly that they assembled into aggregates (Figure 5e) even when $\rho_{PDMS} = \rho_{H_2O}$. We developed a new method to generate hexagons with smooth bottom faces for these experiments; details can be found in the Supporting Information.
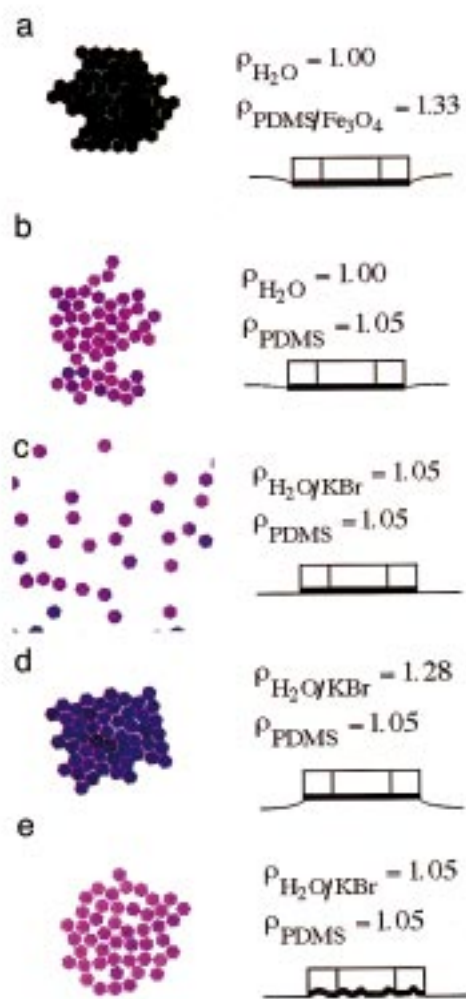
Figure 5. Assembly of [0] hexagons. All of the densities are in g/cm^3. In (a) the hexagons sank into the PFD/H_2O interface and formed a close-packed array. (b) Hexagons were only slightly denser than the water and barely perturbed the interface. (c) Densities of the PDMS and water were matched and the objects floated on the interface without menisci. (d) PDMS was less dense than the water, and a positive meniscus formed at the interface. (e) Hexagons that were generated by cutting the bottom face with a razor blade had a rough intersection between the bottom face and the side faces, and micromenisci formed that caused the hexagons to assemble even when $\rho_{PDMS} = \rho_{H_2O}$. The density of PFD is 1.91 g/cm^3.

To demonstrate the influence of the relative density of PDMS and water on the behavior of the system, we allowed the [0] hexagons to aggregate in systems having aqueous phases of different density. The hexagons in Figure 5b had small negative menisci; the attraction between the hexagons was too small to form an ordered array if there was any agitation but was strong enough to cause the hexagons to aggregate into loose arrays when agitation had stopped. The hexagons in Figure 5c had no menisci. We matched the density of the PDMS and water by adding KBr to the water. The hexagons showed no tendency to aggregate. The hexagons in Figure 5d had positive menisci. The density of the water was adjusted to a value ($\rho = 1.28$ g/cm^3) that was *greater* than that of the PDMS. In this experiment, the hexagons were lighter than the water and rose, but they remained pinned to the PFD/H_2O interface by the PFD wetting their bottom faces. A small positive meniscus of PFD formed at the faces of the hexagons, and the resulting capillary forces were

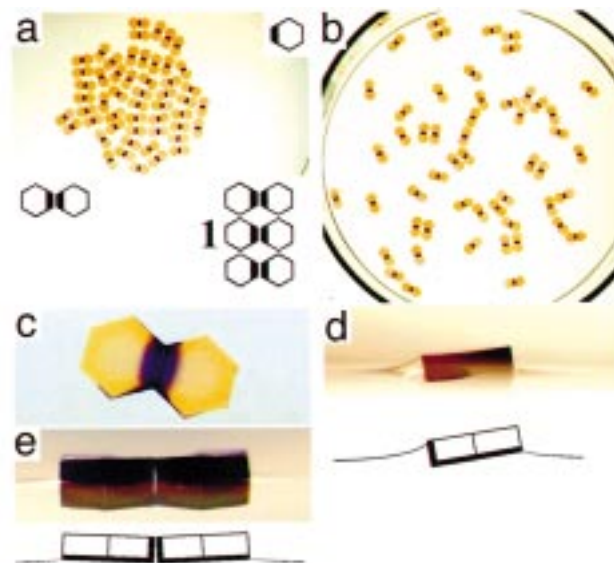**Figure 6.** Close-packed array formed by assembly of [1,2,3,4,5,6] hexagons.

Figure 7. Assemblies that form by aggregation of [1] hexagons. (a) Aggregates of dimers that formed after agitation stopped. (b) Dimers after being separated by hand. (c) Close-up of a dimer shows the registration between the hydrophobic faces. (d) [1] Hexagon from the side shows the large positive meniscus on the left-hand side of the hexagon (the [1] face) and a small, positive meniscus on the right-hand side of the hexagon (the 4 face) due to the tilt of the hexagon at the interface. (e) Hexagons, after assembling into a dimer, were still tilted at the interface.
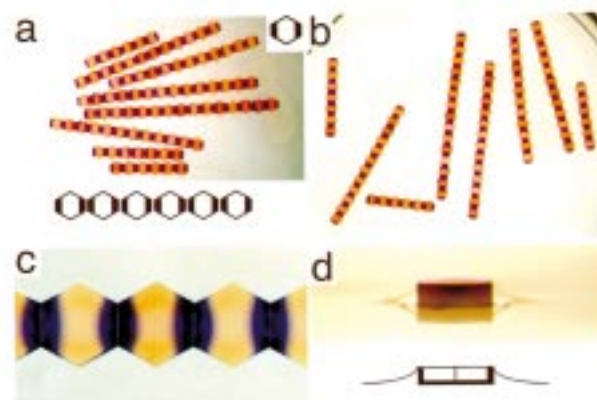
Figure 8. Assemblies from the [1,4] hexagons. (a) Lines aggregated loosely after agitation stopped. (b) Lines after being separated by hand. (c) Close-up of a line shows the registration between the hydrophobic faces. (d) Side view shows the menisci on the hydrophobic faces; the hexagon appears thicker than its actual size because of a reflection at the interface.

sufficiently strong to allow a close-packed array of hexagons to assemble that survived under mild agitation ($\omega = 0.75$ s^{-1}). In all of these systems, the capillary forces holding the arrays together were weaker than those between two hydrophobic faces of hexagons with comparable dimensions.

These experiments demonstrate the important fact that the hydrophilic faces of the hexagons *can* interact, albeit weakly, through either negative or positive menisci. The density of the aqueous phase ranged from slightly less than that of PDMS to substantially greater than that of PDMS, while the PFD/H$_2$O interfacial free energy remained relatively unchanged.[62] The variation in density changed the sense and size of the menisci and thus the strength of the attractive interaction between the hexagons. The observation that aggregates formed when $\rho_{PDMS} > \rho_{H_2O}$ and $\rho_{PDMS} < \rho_{H_2O}$ but not when $\rho_{PDMS} = \rho_{H_2O}$ confirmed that both positive and negative menisci led to similar structures and that elimination of the menisci eliminated the attraction among the hexagons.
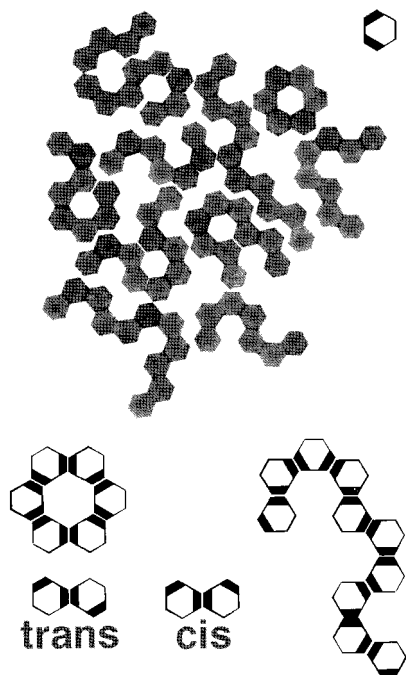
[1,2,3,4,5,6] Hexagons. These hexagons formed close-packed arrays (Figure 6). The hexagons were placed on the surface and agitated at $\omega = 0.75$ s^{-1}; one or two arrays self-assembled. At higher rates of agitation, $\omega = 1.0$ s^{-1}, two to four arrays formed. At even higher rates of agitation, $\omega = 1.5$ s^{-1}, numerous arrays formed.

[1] Hexagons and [1,4] Hexagons. The [1] hexagons formed dimers (Figure 7), and the [1,4] hexagons formed linear arrays ("lines"; Figure 8), both as expected. Both dimers and lines formed rapidly (assembly was complete in less than 30 min). The length of the lines formed by the [1,4] hexagons depended on the rate of agitation. The assembly in Figure 8a, b was assembled by first agitating at $\omega = 1.5$ s^{-1} for 10 min; when the rate of agitation was decreased to 1.0 s^{-1} for 20 min, longer (5–15 hexagons) lines assembled by coalescence from the shorter lines (3–7 hexagons).

Figure 7 shows five views of the arrays formed by the [1] hexagons, and Figure 8 shows four views of the arrays formed by the [1,4] hexagons. We learned four important points from these assemblies. (i) The alignment between the hydrophobic faces was excellent. The hydrophobic faces moved relative to one another so that they came into contact with their faces opposed to one another. (ii) The unassembled [1] hexagon and the two [1] hexagons self-assembled into a dimer are tilted, but the unassembled [1,4] hexagons are not tilted. The unassembled [1] hexagon is tilted less than the dimer of the hexagons. (iii)

(62) Aveyard, R.; Saleem, S. M. *J. Chem. Soc., Faraday Trans. 1* **1976**, *72*, 1609–1617.

The dimers tended to aggregate into ordered structures, **1**, through the negative menisci on the hydrophilic faces. The strength of the interaction between the hydrophilic faces was too small to self-assemble the dimers into ordered arrays. The interactions between the hydrophilic faces on the [1,4] hexagons were too small to self-assemble the lines into ordered arrays. (iv) The size of the lines was limited by the strength of the agitation (as we have already described).

[1,3] Hexagons. Our initial expectation was that this system might generate a cyclic structure containing six hexagons. In principle, a cyclic array would satisfy all of the hydrophobic faces and form a compact aggregate that would resist disruption by shear. In fact, the arrays formed by the [1,3] hexagons contained few cyclic hexamers and consisted primarily of long,

Figure 9. [1,3] Hexagons (1.0-mm thick) self-assembled into an unordered array. Although cyclic hexamers formed occasionally, they rapidly broke apart under agitation. This set of aggregates has only one cyclic hexamer (upper right-hand corner) that juxtapose only hydrophobic faces.

kinked lines connected through the hydrophobic faces (Figure 9). We examined [1,3] hexagons having different (0.9−2.0 mm) heights, but at no height did the assembly result in extensive formation of ordered arrays. For 1.2-mm thick hexagons, high rates of agitation ($\omega = 1.5$ s^{-1}) favored small arrays. Much less than one-half of the hexagons assembled into cyclic hexamers at $\omega = 1.5$ s^{-1}; when the agitation was slowed to $\omega = 1.0$ s^{-1}, the assembly became irreversible, and the [1,3] hexagons coagulated into the disordered arrays similar to those in Figure 9. We infer that there is little difference in energy between the "cis" and "trans" configurations of these systems and that none of the other influences that might have favored either cyclic hexamers or meandering linear arrays—for example shear forces or interactions between negative menisci—were significant.

We wanted to test whether the observed arrays were an artifact of the starting conditions; in particular, we wished to ensure that the nearly complete absence of cyclic hexamers accurately reflected their stability during the agitation. To test the stability of the cyclic hexamers, we assembled 14 cyclic hexamers (1.0-mm thick) by hand at the PFD/H$_2$O interface. We agitated this system at $\omega = 1.5$ s^{-1} (unordered [1,3] hexagons reversibly assembled into cyclic hexamers at this rate of agitation). The cyclic hexamers rapidly broke up into small unordered arrays as before. The results of the assembly were thus the same whether the starting point was an unordered collection of monomers and aggregates or ordered, cyclic hexamers.

We repeated this experiment starting with 14 cyclic hexamers assembled with 1.6-mm thick hexagons. These hexagons had higher positive menisci and were attracted to one another more strongly than the 1.0-mm thick hexagons. These hexagons did not dissociate even at the highest rates of agitation ($\omega = 1.5$ s^{-1}) over a period of hours. Hexagons that were 1.6-mm thick and unordered prior to agitation assembled into arrays similar to those in Figure 9. The results of the assembly for 1.6-mm

thick hexagons thus depended on the starting point, since cyclic hexamers, once formed, were kinetically stable.

[1,2] Hexagons (1.2-mm Thick). In principle, the [1,2] hexagons could form trimers or parallel lines; under the conditions used ($\omega = 1.5$ s^{-1}), they formed only trimers (Figure 10). These trimers were stable and did not break apart even at the highest rate of agitation ($\omega = 1.5$ s^{-1}). Both trimers and lines juxtapose hydrophobic faces.

To test the relative stability of the trimers and parallel lines (arrays **2** and **3**, Figure 10a), we assembled eight hexagons by hand into an array in the form of **3** and agitated the system in the presence of trimers. The parallel lines were stable over a period of hours at $\omega = 1.5$ s^{-1}. We infer, from this observation, that the preference of the system for trimers from separated [1,2] hexagons reflects kinetic factors rather than relative stabilities, but we do not, in fact, know which form is more stable.

In inquiring why the [1,2] hexagons formed trimers rather than lines, we observed that when two hexagons came into proximity, they would rotate and orientate so that they came into contact in the correct orientation to form a trimer but *not* a linear array: that is, the preference for trimers rather than lines was already evident at the level of dimers (Figure 11a). When we placed two hexagons by hand in the correct orientation to form lines (**3**, Figure 10), the hexagons readily dissociated and reassembled in the orientation required for trimers. We believe that the origin of these differences is the pronounced tilt of the [1,2] hexagons with respect to the interface ($14 \pm 1°$, Table 1), the structure of the menisci that followed from this tilt, and the requirement that the contours of menisci on juxtaposed faces of adjacent hexagons be matched for stability. When two hexagons assembled in the orientation to form a trimer, the contours of the menisci on the two interacting faces matched (Figure 11a). When two hexagons assembled in the orientation required to form a line, the contours of the menisci of the two interacting faces did not match (Figure 11a). Matching the contours of the interacting menisci yielded the lower PFD/H$_2$O interfacial area in the dimer and thus the lower energy. Interestingly, the [1,2] hexagons that had assembled into a trimer were still tilted relative to the interface (Figure 10d). The tilt did not disappear even after all of the hydrophobic faces were juxtaposed.

[1,2] Hexagons (2.0-mm Thick). The trimers formed by the 2.0-mm thick [1,2] hexagons self-assembled into larger arrays at low rates of agitation (Figure 10e). The trimers formed from the 1.2-mm thick hexagons tended to assemble into larger arrays, but these arrays were not ordered (Figure 10a). We hypothesized that if the hexagons were thicker (here, 2.0 mm), they would be more strongly tilted at the interface than the 1.2-mm thick hexagons. As a result, larger positive menisci would exist on the 4 and 5 faces, and there would be a greater tendency for the thicker trimers to form structured arrays than for the thinner trimers to do so. In fact, the menisci at the 4 and 5 faces were sufficiently large to cause the trimers to assemble into ordered arrays at low rates of agitation.

The 2.0-mm thick [1,2] hexagons were strongly tilted before and after self-assembling into trimers (Figure 10g, h). These [1,2] hexagons formed primarily trimers, although structures such as **4**—in which the four exposed hydrophobic faces are sufficiently close to interact through capillarity—were also stable for extended periods of time at $\omega = 1.5$ s^{-1}.

These aggregates of the trimers were notable for three reasons. (i) They are an example of hierarchical self-assembly. The [1] and [2] faces were strongly attracted to one another through large, positive menisci; the hydrophilic 4 and 5 faces were
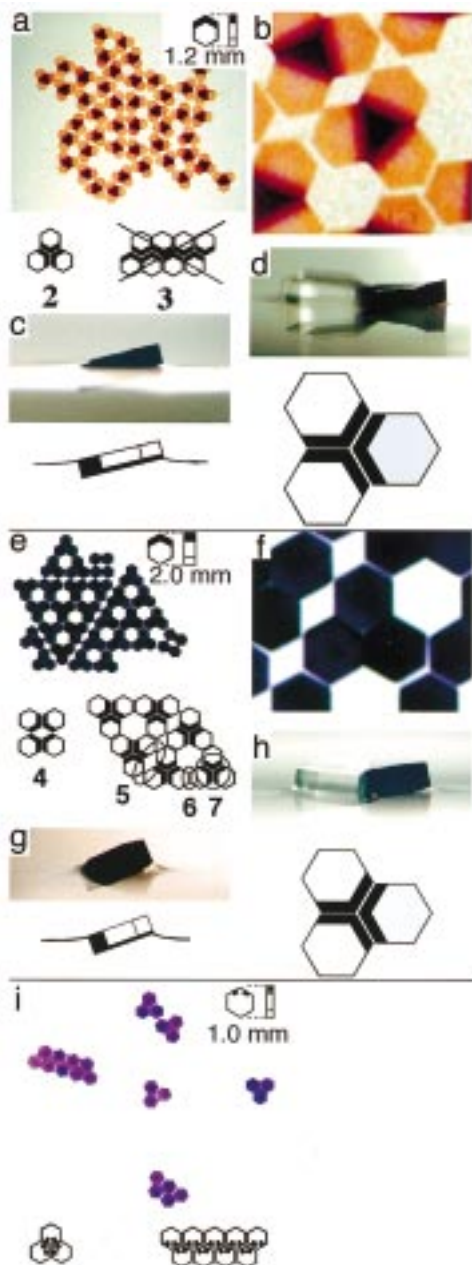
Figure 10. (a) [1,2] Hexagons (1.2-mm thick) formed trimers exclusively. (b) Trimers aggregated with one another loosely when the agitation was weakened. (c) Optical micrographs of the hexagons from the sides shows both the tilt and the positive meniscus along the intersection of the 4 and 5 faces that are pulled out of the interface by the tilt. (d) Trimer, viewed from the side, shows that the hexagons were still tilted. Trimer in this image was assembled from one dark hexagon (on the right) and two transparent hexagons (on the left). The dark hexagon is orientated as in (c). The dark faces on the hexagons in (a) and (b) are hydrophobic. (e) and (f) Trimers were the principal aggregates from the assembly of the 2.0-mm thick hexagons; these trimers (and occasionally structures such as **4**) assembled further into larger aggregates when the agitation was weakened. (g) Hexagons from the sides show both a tilt and a positive meniscus along the intersection of the 4 and 5 faces; these faces are pulled out of the interface by the tilt. (h) Trimer from the side shows that the hexagons were still tilted. Trimer in this image was assembled from one dark hexagon (on the right) and two transparent hexagons (on the left). The dark hexagon is orientated as in (g). (i) [$1_{1:2:1}$,$2_{1:2:1}$] Hexagons (1.0-mm thick) assembled into both lines and trimers.

weakly attracted to one another through the smaller menisci formed as a result of the tilt of the hexagons. (ii) The hexagons in the trimers self-assembled into close contact (**7**, Figure 10), but the trimers self-assemble at a greater distance (**6**, Figure 10); there remained a small but easily perceptible separation

between the 4 and 5 faces on separate trimers. (iii) The trimers sometimes assembled into structures (**5**, Figure 10) in which the closest contact was between *vertexes* rather than faces. This structure is an example of a vertex-to-vertex assembly; other examples appear in later sections.

[$1_{1:2:1}$,$2_{1:2:1}$] Hexagons (1.0-mm Thick). Faces Only Partly Wettable by PFD. We hypothesized that the origin of the preference of [1,2] hexagons to form trimers lay in their tilt at the PFD/H$_2$O interface. To test this hypothesis, we examined the aggregation of [$1_{1:2:1}$,$2_{1:2:1}$] hexagons (1.0-mm thick). In these hexagons, the hydrophobic area per face was one-half of that of the [1,2] hexagons, and the size and shape of the menisci on these faces do not tend to tilt the hexagons out of the plane of the PFD/H$_2$O interface (Table 1).[63] Aggregation of the [$1_{1:2:1}$,$2_{1:2:1}$] hexagons led to both trimers and lines (Figure 10i) at $\omega = 1.5$ s^{-1} where the assembly was reversible. The partly hydrophobic faces of the [$1_{1:2:1}$,$2_{1:2:1}$] hexagons were attractive toward one another (albeit more weakly than the [1,2] hexagons), but because there was little tilt, there was no preference for orientation at the dimer stage, and both trimers and lines ultimately formed. This system also had little tendency to aggregate further into larger arrays on the basis of interactions between the hydrophilic faces.

These results provide further support for the hypothesis that the tilting of the hexagons at the PFD/H$_2$O interface strongly influences their assembly.

[1,3,5] Hexagons. The [1,3,5] hexagons assembled into an open array (Figure 12). When a system of 130 [1,3,5] hexagons was agitated at $\omega = 1.5$ s^{-1}, several open hexagonal arrays assembled; when the intensity of agitation decreased, these arrays aggregated without breaking any of the existing hydrophobic/hydrophobic interactions.[64] We could not anneal a system of several small arrays into one single array. In a system with fewer [1,3,5] hexagons ($\sim$80), the hexagons self-assembled into one large array (Figure 12).

[1,2,3] Hexagons (1.2-mm Thick). These hexagons assembled into a mixture of cyclic hexamers and other structures (Figure 13). These hexagons were tilted by $15 \pm 1°$ with respect to the interface (Table 1), and the [2] face was essentially completely immersed in the PFD, with only a small residual positive meniscus (Figure 13c). The primary products of the assembly were cyclic hexamers **8**, dimers **9**, trimers **10**, tetramers **11**, and lines **12**. The hexagons assembled into the remarkable line motif, **12**—a *vertex-to-vertex* array—with their hydrophobic faces orientated along the same side of the line. These lines were not rigid; they flexed readily, and the lines folded up into cyclic arrays. At any time, about one-half of the hexagons present in the system were present as cyclic hexamers. We have not identified conditions that generated *only* cyclic hexamers.

The [1,2,3] hexagons did not interact through the [2] face because this face was essentially buried below the mean plane of the PFD/water interface (Figure 13c). Because the [2] face was invisible, the [1,2,3] hexagons and the [1,3] hexagons had, in a sense, similar patterns of hydrophobic faces, and both assembled on the basis of interactions between the [1] and [3] faces. The difference between the [1,3] and [1,2,3] hexagons

(63) Tilting the hexagons would decrease the positive menisci [$1_{1:2:1}$] and [$2_{1:2:1}$] faces, but increase the negative ones on the [$1_{1:2:1}$] and [$2_{1:2:1}$] faces; these effects partially off-set each other and result in little tendency for these faces to be pulled into the plane of the interface.

(64) There was a limit to the size of the array that could be formed at any given level of agitation due to the shear forces across the aggregate caused by the circular agitation. The shear forces were strongest on the hexagons at the outer edge of the array, and high rates of agitation separated these hexagons from the array.
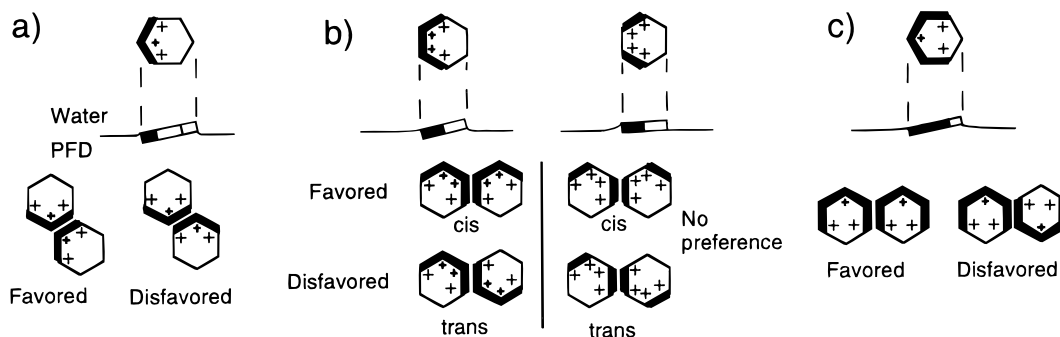
Figure 11. Contour of the menisci along the hydrophobic faces was determined by the tilt of the hexagon. Shape of the meniscus is indicated by the + symbol; the larger this symbol, the higher the meniscus is at that point on the face. (a) Two ways to form a dimer of the [1,2] hexagons. In the favored configuration, the contours of the positive menisci along the faces match; in the unfavored configuration, the contours do not match. (b) Contour of the menisci along the [1] and [3] faces of the [1,2,3] hexagons is unsymmetrical about the center of the face as a result of the tilt of the hexagons. Meniscus is high at the intersection of the [1] and 6 faces and the [3] and 4 faces; only the cis configuration matches the contours of the menisci well. [1,3] Hexagons floated approximately parallel to the interface, and the height of the menisci along these faces is nearly constant; both the cis and trans configurations match the contours of the menisci well. (c) [1,2,3,4] Hexagons were strongly tilted at the interface. Hexagons assembled to match the contours of the menisci on the opposing faces.
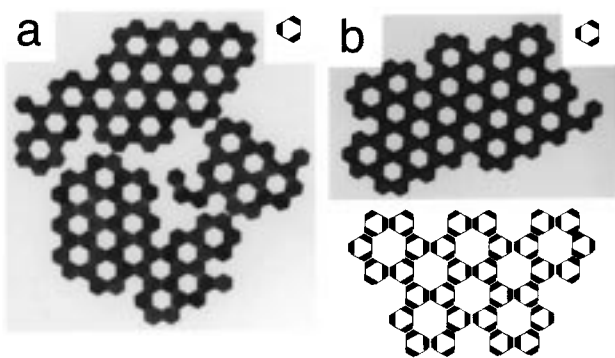
Figure 12. [1,3,5] Hexagons formed one or more open, hexagonal arrays.

was that the latter was more strongly tilted and the contours of the menisci varied much more along the [1] and [3] faces on the [1,2,3] hexagons than on the [1,3] hexagons (Figure 11b). The [1,3] hexagons dimerized into both cis and trans configurations; the [1,2,3] hexagons yielded only the cis configuration.

The significance of these observations is their demonstration that the tilting of the [1,2,3] hexagons was important in determining the structures of the aggregates that formed. The tilt of the [1,2,3] hexagons provided a directionality to the assembly that the [1,3] hexagons lacked. The favored configuration was that that matched the shape of the menisci on the hydrophobic faces. In the [1,2,3] hexagons, the menisci on the [1] and [3] faces were asymmetric around the middle of the face as a result of tilt and required a matching tilt between the hexagons on assembly. In the [1,3] hexagons, the menisci on the [1] and [3] faces were approximately symmetrical around the middle of the face and allowed two configurations for the dimers.

[1,2,3] Hexagons (2.0-mm Thick). Two different types of aggregates formed commonly from the 2.0-mm thick [1,2,3] hexagons (Figure 13). Cyclic hexamers, **8**, formed (as they did with the 1.2-mm thick hexagons); the line, **12**, also formed. Again, the [2] face was not, in general, in contact with other faces.

The 2.0-mm thick [1,2,3] hexagons were tilted by $30 \pm 1°$ relative to the interface (Table 1; this angle of tilt was the largest that we have observed). Both the hydrophobic [2] face and the hydrophilic 5 face had small, positive menisci (Figure 13); the [2] face had a positive meniscus because it was hydrophobic, the

and the 5 face had a positive meniscus because it was tilted out of the PFD/H$_2$O interface. One reason for the stability of the cyclic hexamer was that the contours of the positive menisci along the [1] and [3] faces of the hexagons were matched in this configuration. The hexagons in the lines, **12**, also interacted by matching the contours of their menisci. The line motif is one of several configurations in which the closest contacts involved vertexes rather than faces (see also Figures 10 and 15), but it is unique in its flexibility.

[$1_{1:2:1}$,$2_{1:2:1}$,$3_{1:2:1}$] Hexagons (1.2-mm Thick). We fabricated these hexagons to confirm that the arrays formed by the other [1,2,3] hexagons were strongly influenced by the tilting of their constituent hexagons relative to the plane of the interface. The [$1_{1:2:1}$,$2_{1:2:1}$,$3_{1:2:1}$] hexagons were not appreciably tilted ($5 \pm 2°$, Table 1). These hexagons rapidly assembled into quasi-ordered arrays having two characteristics (Figure 13): (i) Because these hexagons were not significantly tilted, the [$2_{1:2:1}$] faces were exposed and interacted with other partially hydrophobic faces, and (ii) most of the half-hydrophobic faces were in contact with other half-hydrophobic faces, although some hexagons assembled into configurations where a half-hydrophobic face was in contact with a hydrophilic face. We do not understand why some half-hydrophobic faces assembled opposed to a fully hydrophilic face, but we noted that these hexagons always had at least one other half-hydrophobic face in contact with another half-hydrophobic face; i.e., the hexagons had at least one attractive interaction between hexagons in the array.

[1,2,4] Hexagons and [1,2,5] Hexagons. Chiral Systems. The [1,2,4] and [1,2,5] hexagons are chiral and enantiomeric to one another, and the arrays formed by these two types of hexagons were mirror images of one another (Figure 14). The predominant structure formed was short lines composed of parallel, interacting sets of hexagons; over one-half of these hexagons joined these aggregates. The rest were present in aggregates that seemed to extend the line motif to three rows, fragments of the two types of lines, or unordered aggregates.

Two distinct types of arrays formed. One (**13** or its enantiomer **13'**) is coplanar with the PFD/H$_2$O interface; the second (**14** and **14'**) is tilted with hexagons at one face pulled into the PFD phase by capillary forces. Both arrays were stable at $\omega = 1.5$ s^{-1}. Although **14** and **14'** had exposed hydrophobic faces, they did not dimerize under these conditions: these exposed faces were tilted far into the PFD/H$_2$O interface and had only small
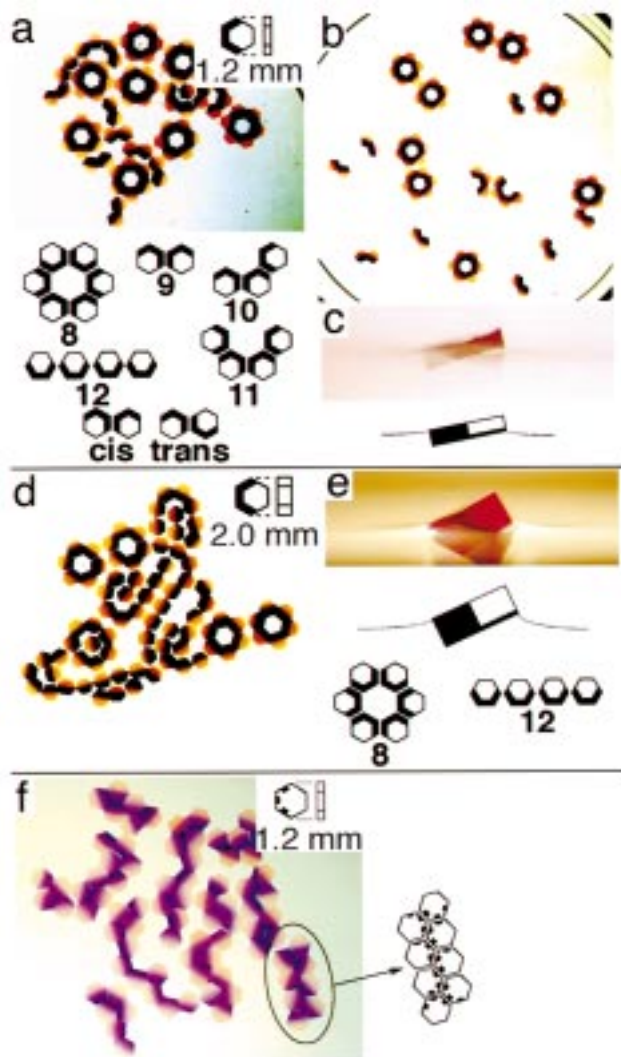
Figure 13. (a) [1,2,3] Hexagons (1.2-mm thick) assembled into lines, cyclic hexamers, tetramers, trimers, and dimers. The aggregates that formed after the agitation was stopped showed weak interactions between the structured arrays. The dark faces on the hexagons are hydrophobic. (b) Arrays, after being separated by hand, show the aggregates stable to the agitation. (c) [1,2,3] Hexagon from the side shows a small, positive meniscus on the hydrophilic 5 face; this face is tilted out of the interface. (d) [1,2,3] Hexagons (2.0-mm thick) assembled into cyclic hexamers and aggregates based on the line motif, **12**, in which the hexagons assembled at the vertexes between the [3] and 4 and the [1] and 6 faces. (e) Optical micrograph of the [1,2,3] hexagon from the side shows the positive menisci along the 5 face and the nearly completely immersed [2] face. (f) [$1_{1:2:1}$,$2_{1:2:1}$,$3_{1:2:1}$] Hexagons (1.2-mm thick) assembled into quasi-ordered arrays. Hydrophobic faces assembled predominately with hydrophobic faces, but a number of configurations are apparently accessible.

positive menisci. We cannot presently rationalize the formation of two different arrays (e.g., **13** and **14**) having structures that are overall so similar.

We assembled arrays from a racemic mixture of [1,2,4] and [1,2,5] hexagons (Figure 14d). The arrays that self-assembled from the racemic mixture were different from the arrays that self-assembled from the [1,2,4] and [1,2,5] hexagons individually. The racemic mixture assembled into arrays based primarily on the two different types of the trimers shown in Figure 14d. The trimers self-assembled with the circled parts conserved, but the pattern of the remaining hydrophobic faces was not well
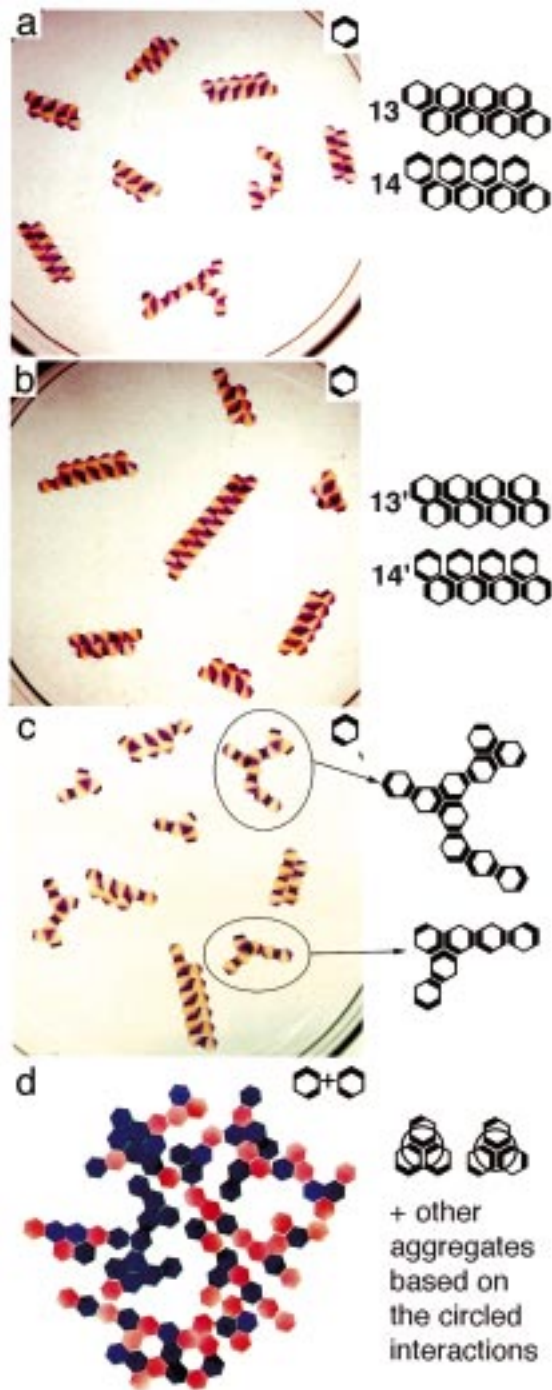
Figure 14. Arrays formed from the [1,2,4] hexagons (a) and the [1,2,5] hexagons (b) and (c). Both hexagons are chiral, and both assembled into arrays; these arrays are mirror images of one another. The dark faces are hydrophobic and the light faces are hydrophilic. (b) This optical micrograph is an example of the most homogeneous ordered assembly of the [1,2,5] hexagons. (c) Results of these assemblies often contained unordered aggregates; this optical micrograph is representative of the types of arrays that we often observed. (d) Aggregates that self-assembled from a racemic mixture of the [1,2,4] and [1,2,5] hexagons are shown. The [1,2,4] hexagons are dark and the [1,2,5] hexagons are light. Many different arrays assembled, but the trimers shown were common repeating units. The circled regions of the trimers in the inset were conserved in the arrays; the pattern of the remaining hydrophobic faces differed.

controlled. The trimers assembled rapidly (∼5 min at $\omega = 1.5$ s^{-1}), and these trimers then more slowly (∼30 min) assembled into larger aggregates.
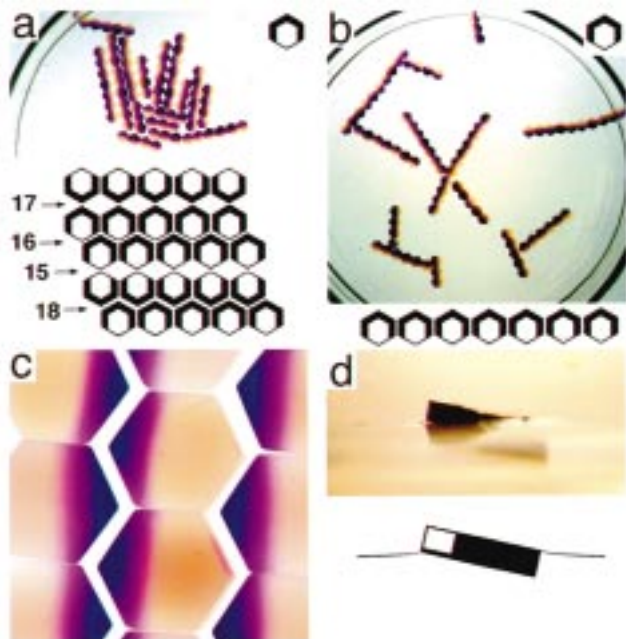
Figure 15. Array of the [1,2,3,4] hexagons as they appeared after the agitation was stopped (a) and after separating the lines by hand (b). (c) Close-up of the interacting lines shows a small separation. This separation is in contrast to the close contact of the hexagons in the lines. (d) [1,2,3,4] Hexagon from the side confirms a pronounced tilt of the hexagons at the interface.

[1,2,3,4] Hexagons. The arrays formed by the [1,2,3,4] hexagons left one-half of the hydrophobic faces exposed (Figure 15); again, the tilting ($14 \pm 1°$, Table 1) of the individual hexagons relative to the plane of the interface buried these unpaired hydrophobic faces in the PFD phase. After assembling into the linear array, the hexagons remained tilted with an angle similar to that of the free, isolated hexagons.

The [1,2,3,4] hexagons (both 1.0- and 2.0-mm thick) formed lines with the hexagons tilted in the same orientation in the array: the [2] and [3] faces were pulled the furthest into the PFD. The heights of the menisci on the [1] and [4] faces were small near the intersection with the [2] and [3] faces and large near the 6 and 5 faces, respectively (Figure 11c). Small positive menisci formed along the intersection of the 5 and 6 faces where the hexagons were pulled out of the interface. We believe that the difference in heights of the menisci along the [1] and [4] faces and the weak interaction between the [2] and [3] faces on adjacent hexagons oriented the hexagons in the lines.

The lines interacted weakly during the agitation. When the agitation was slowed to $\omega = 0.5$ s^{-1}, the lines assembled into the arrays shown in Figure 15a. The hydrophilic faces had small, positive menisci due to the tilt of the hexagons at the interface (Figure 15d). The exposed hydrophilic faces interacted with one another by vertex-to-vertex contacts (**15**), the exposed hydrophobic faces interacted with the hydrophilic faces by face-to-face contact (**16**), and the exposed hydrophobic faces interacted with one another through the vertex-to-vertex (**17**) or face-to-face (**18**) contacts.

In the aggregates characterized by face-to-face interactions (**16** and **18**), the faces did *not* come into close contact; instead, they maintained a short separation (<1 mm) from one another. This separation between two interacting faces was similar to the separation between the trimers of the [1,2] hexagons (Figure 10).

[1,2,4,5] Hexagons. When agitated at $\omega = 1.5$ s^{-1}, the [1,2,4,5] hexagons assembled into an open, hexagonal array
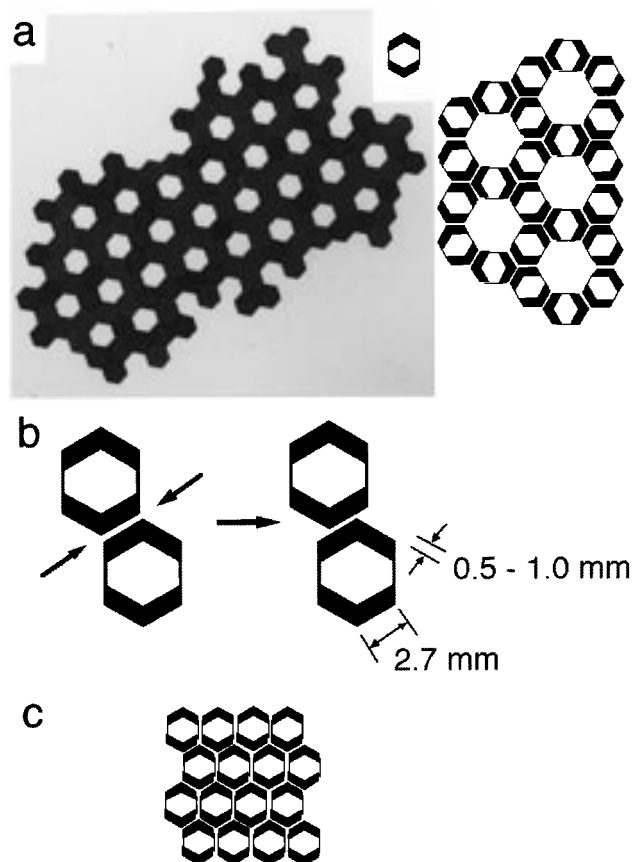
Figure 16. (a) Assembly of [1,2,4,5] hexagons resulted in an open, hexagonal array. (b) Two hexagons were assembled by hand as shown; they moved laterally by 0.5–1.0 mm when released. Arrows point to the areas between the hexagons where a negative meniscus is close to a positive meniscus. (c) Close-packed arrangement of hexagons did not form spontaneously but was stable to the agitation if formed by hand.
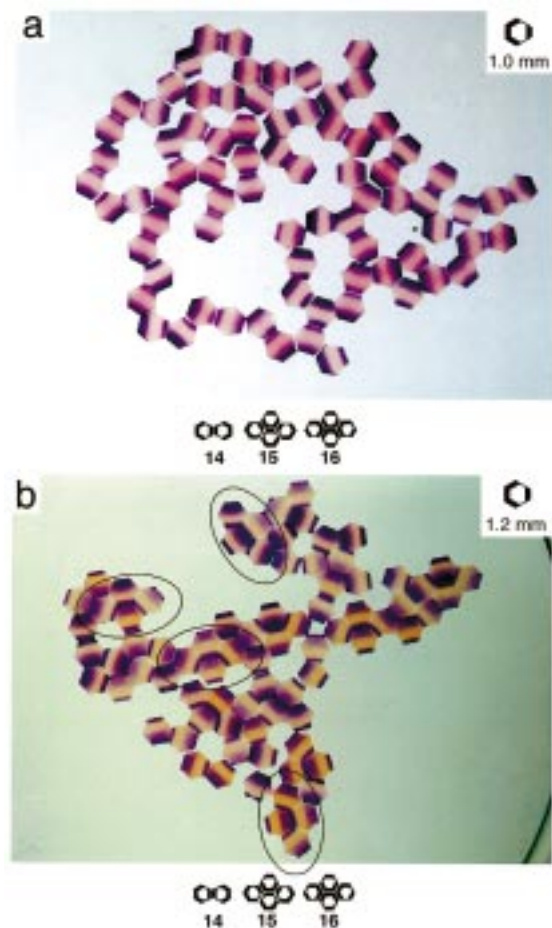
(Figure 16). This array was the only aggregate stable at $\omega = 1.5$ s^{-1}. The hexagons floated parallel to the interface, although they were pulled into the PFD/H$_2$O interface (by an estimated 0.65 mm for a 1.2-mm thick hexagon isolated at the interface; Table 2).

In exploring other assemblies, we placed two hexagons by hand into the orientation shown in Figure 16b; from the orientation with the faces fully aligned, the hexagons spontaneously moved laterally by approximately 20–40% of the width of the face. We believe that this movement was caused by the interaction of the positive menisci at the hydrophobic faces and the negative menisci at the hydrophilic faces, but we have not modeled the interaction in detail. This dimer was only weakly stable.

We assembled arrays with 16, 9, and 4 hexagons into the configuration shown in Figure 16c and agitated them in the presence of free hexagons and hexagons in an open array at $\omega = 1.5$ s^{-1}. These arrays were stable to the agitation for a period of hours. The result of the interaction shown in Figure 16b and the stability of the close-packed arrays shown in Figure 16c indicates that the open array of [1,2,4,5] hexagons is a product of kinetic assembly but may not be the most stable product.

[1,2,3,5] Hexagons. The [1,2,3,5] hexagons formed different arrays, depending on their thicknesses. For assemblies carried out using hexagons less than 1.2-mm thick, we often observed loose structured arrays of the type shown in Figure 17a. The hexagons self-assembled ($\omega = 1.5$ s^{-1}) into dimers, **14**, and

Figure 18. (a) Typical array assembled from the [1,2,3,4,5] hexagons. The dark faces are hydrophobic. (b) Isolated [1,2,3,4,5] hexagon from the side shows a pronounced tilt. (c) A dimer of hexagons—assembled with their hydrophilic faces in contact—shows the hexagons were still tilted after assembly.

[1,2,3,4,5] Hexagons. We observed no ordered arrays in the assembly of the [1,2,3,4,5] hexagons (Figure 18). The hexagons displayed a preference to assemble with their hydrophilic faces either adjacent to one another or in contact. Isolated hexagons at the interface were tilted by $9 \pm 2°$ (Table 1, Figure 18b); a dimer of the [1,2,3,4,5] hexagons assembled with hydrophilic faces in contact was tilted by $6 \pm 1°$ at the interface (Table 1, Figure 18c). We examined the structures formed by the assembly of hexagons with heights from 1.0 to 2.0 mm, and observed similar patterns for all of them.

Capillary Forces

This section summarizes the basic equations describing the menisci, and the boundary conditions used to solve these equations, using two model systems, an isolated, infinitely long face, and two infinitely long faces that interact through menisci. It also analyzes the gravitational and capillary energies of the latter system as a function of the distance between the faces. We use our understanding of how the capillary energies scale with the dimensions of the objects to estimate how far hexagons with centrosymmetric patterns of hydrophobic faces are pulled into the PFD/H$_2$O interface by the vertical component of the capillary forces. There are a number of excellent papers on capillary forces that derive these equations in detail.[40,43−46]

The shape of the meniscus is described by the Laplace equation of capillary hydrostatics (eq 1).

$$\frac{\gamma \frac{d^2 h}{dx^2}}{\left(1 + \left(\frac{dh}{dx}\right)^2\right)^{3/2}} = \Delta\rho g h - \Delta P_0 \qquad (1)$$

Here, h (m) is the height of the meniscus at point x, γ (J m^{-2}) is the interfacial free energy of the PFD/H$_2$O interface, $\Delta\rho$ (kg m^{-3}) is the difference in density between the PFD and water, g (m s^{-2}) is the acceleration due to gravity, and ΔP_0 (Pa) is the difference in pressure across the interface. The values for the parameters are: $\gamma = 0.05$ J m^{-2},[55] $\Delta\rho = \rho_{PFD} - \rho_{water} = 1910$ kg m^{-3} − 1000 kg m^{-3} = 910 kg m^{-3}, and $g = 9.81$ m s^{-2}. Equation 1 can be linearized by making the approximation summarized by eq 2, this approximation is valid for contact angles, θ (°), between 55 and 125°.[49]
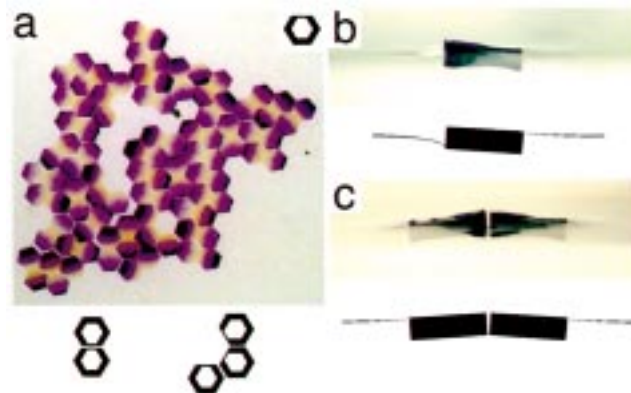

Figure 17. Assembly of [1,2,3,5] hexagons was very sensitive to small differences in thicknesses. (a) Hexagons (1.0-mm thick) self-assembled into various arrays. Several small arrays including the dimer with the [5] faces in contact, **14**, formed at short periods of time; these arrays further assembled as the agitation was continued. (b) Hexagons only slightly thicker (1.2 mm) assembled into larger arrays with common repeating structures such as **14**, **15**, and **16** as common repeating units. We circled examples of **15** in the aggregates.

other arrays; these arrays then condensed into disordered aggregates when the agitation was stopped. When the hexagons were self-assembled with weaker agitation ($\omega = 1.0$ s^{-1}), arrays such as **14**, **15**, and **16** were stable. For hexagons that were 1.2-mm thick, we observed arrays such as those shown in Figure 17b. The smaller arrays **14**, **15**, and **16** had further aggregated into larger arrays. The arrays that self-assembled from the 1.0-mm thick hexagons ($\omega = 1.0$ s^{-1}) and 1.2-mm thick hexagons ($\omega = 1.5$ s^{-1}) were similar to one another in the types of arrays that formed, but the arrays that assembled from the 1.2-mm thick hexagons further assembled into larger arrays.

For hexagons thicker than 1.2 mm, the menisci on the [5] faces were not present at all times. The PFD dewet from the [5] face during the agitation and did not reform. These hexagons were tilted strongly at the interface with the [2] face almost buried into the interface and the [5] face above the interface. In several experiments we placed the hexagons at the interface so that all of the [5] faces had positive menisci, the hexagons were agitated at $w = 1.5$ s^{-1}, the agitation was stopped (usually after 30 min), and the arrays were characterized. Some of the hexagons had assembled with the [5] face in contact with other hydrophobic faces, but most of the exposed [5] faces did not have positive menisci. For hexagons thicker than 1.2 mm, the tilt of the hexagons at the interface made the menisci along the [5] face unstable to the agitation.

$$\frac{\dfrac{d^2h}{dx^2}}{\left(1+\left(\dfrac{dh}{dx}\right)^2\right)^{3/2}} \approx \frac{d^2h}{dx^2} \tag{2}$$

We examined the contact angles in our system to decide whether we can use the linear approximation in eq 2. The contact angles differed for the undyed and dyed PDMS (Table 3). Although some of the contact angles fall outside of the range for the linear approximation, we will use the linearized form of the Laplace equation for the rest of our calculations for three reasons. (i) The contact angles in our system are close to or inside of the range (55–125°) where the linearized form of the Laplace equation holds and should be describable semiquantitatively if not quantitatively.[49] (ii) The solutions to the linearized form of the Laplace equation are easier to interpret and understand than those from the nonlinearized Laplace equation. (iii) For heights of the objects in which we are interested (<1.2 mm), the nonlinear Laplace equation simplifies to the linear Laplace equation. With the approximation of eq 2, eq 1 can be simplified to eq 3.

$$\frac{d^2h}{dx^2} = \frac{1}{\gamma}(\Delta\rho gh - \Delta P_0) \tag{3}$$

Equation 3 can be solved for an isolated, infinitely long PDMS face far from any other objects or walls (Figure 19). We will consider the height of the PDMS face to be taller than the height of the meniscus along the face. The two boundary conditions for this problem are that the height of the meniscus goes to zero far from the object, $h(x=\infty)=0$ and that the meniscus makes a constant contact angle at the face of the object $[dh/dx]_{x=0} = -\cot\theta$.[49] The value for ΔP_0 is set equal to zero because the meniscus is flat far from the face. The shape of the meniscus can then be evaluated from eq 3 and the parameters describing the system and is described by eq 4.

$$h(x) = x_C \cot\theta \exp(-x/x_C) \approx$$
$$(2.4 \text{ mm}) \cot\theta \exp(-x/2.4 \text{ mm}) \tag{4}$$

$$x_C = (\gamma/\Delta\rho g)^{1/2} \approx 2.4 \text{ mm} \tag{5}$$

Equation 4 has two important implications. (i) The height of the meniscus decreases exponentially as a function of distance from the hydrophobic face. (The shape of the meniscus is important for understanding how the hexagons interact.) (ii) The decay length, x_C (m), of the exponential describing the menisci in our system (PDMS, H_2O, and PFD) is 2.4 mm. (Objects can interact with one another at several times this length through capillarity.) The maximum height of the meniscus at the face of the objects cannot be predicted using eq 4 because the contact angles of PFD on the dyed PDMS fall out of the region for the linearized form of the Laplace equation. We can get a lower limit for the maximum height of the meniscus at the face of an infinitely long face by using a contact angle of 55° (the limit for the linear Laplace equation); using this value for the contact angle, we estimate that the PFD wets 1.7 mm up the PDMS face. Hexagons that are thicker than the maximum height of the PFD do not increase the extension of the positive menisci, but because the weight of the plates increase, they sink further into the interface under the influence of gravity, and they increase the size and influence of the negative menisci.

For faces with heights, t (m), smaller than the maximum height the PFD can wet the face, the contact angle changes with

Table 3. Contact Angles of PFD on PDMS, Measured with the PDMS Immersed in Water

PDMS	θ_a^{PFD} (deg)	θ_r^{PFD} (deg)
undyed PDMS	41	36
blue PDMS[a]	51	41
red PDMS[b]	62	42

[a] The PDMS was dyed blue by soaking in CH_2Cl_2 with crystal violet overnight. [b] The PDMS was dyed red by soaking in 1/1 EtOH/hexanes containing Sudan red 7B for 8 h.
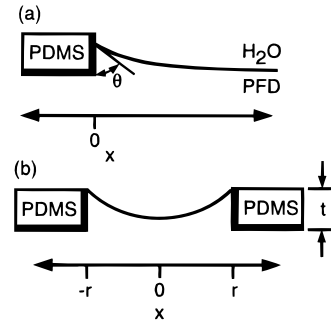
Figure 19. (a) Meniscus on an isolated hydrophobic face follows an exponential decay given by eq 4. (b) Two objects of the same height, t (m), are separated by distance $2r$ (m) and interact through capillarity.
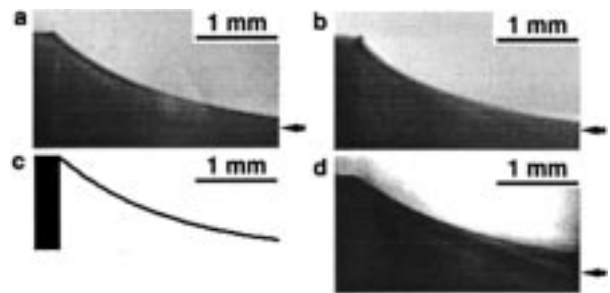
Figure 20. Shape of the menisci: (a) along a hydrophobic face, (b) at the vertex between two hydrophobic faces, and (d) along a PDMS face 16-cm long. The arrows along the edges of the optical micrographs indicate the level of the interface far from the face. (c) Exponential decay with a decay length of 1.2 mm fits the menisci.

the height, and the second boundary condition used to solve eq 3 is not valid. The two boundary conditions used to solve eq 3 in this case are that the height of the meniscus goes to zero far from the object, $h(x=\infty)=0$, and that the meniscus wets the entire face of the object, $h(x=0)=t$. Solving eq 3 with these boundary conditions gives eq 6; this equation describes the menisci for an infinite face with a height less than the maximum height of the PFD, and it is similar to eq 5 except for the preexponential term.

$$h(x) = t \exp(-x/x_C) \approx t \exp(-x/2.4 \text{ mm}) \tag{6}$$

$$\theta = \arctan(x_C/t) \tag{7}$$

The contact angle the PFD makes at the surface of the face is given by eq 7. The value for θ is 55° when the height of the face is 1.7 mm, and the value for θ approaches 90° as t goes to zero. The assumption in eq 2 that was used to linearize the Laplace equation is valid for all heights of the infinitely long PDMS face less than 1.7 mm.

We measured the shape of the menisci along a face and vertex of a [1,2,3,4,5,6] hexagon and in the center of a 16-cm long PDMS face (Figure 20). The menisci along the face and vertex of the hexagon resembled an exponential decay with a decay length of approximately 1.2 mm. The meniscus in the center of

the 16-cm long face had a shape that approximated an exponential decay with a decay length of approximately 1.7 mm. We attribute the differences in the predicted and observed decay lengths to the geometry of the hexagons: the faces of the hexagons were 2.75-mm wide and between 0.9 and 2.0 mm high; these geometries are not well approximated by an infinitely long face. The decay length of the menisci is predicted to decrease as the objects become more removed from the idealized case of the infinitely long face.[65] Ideally, we would solve the Laplace equation for a hexagonal object, but the Laplace equation has not been solved for a geometry of this complexity.[48,66,67] We believe that the solutions for the shapes of the menisci and the energies that we estimate in this paper describe the trends for the menisci and are qualitatively correct for the system of hexagons.

Equation 3 can also be solved for two infinitely long objects of the same height separated by a distance $2r$ (Figure 19b). We assume that the heights of the objects are less than the maximum height of the PFD; most of the objects used in this study fall into this category. The boundary conditions are that the meniscus is flat at the point midway between the objects $(dh/dx)_{x=0} = 0$, and the height of the meniscus at the face of the objects is the height of the objects, $h(x = r) = t$. The value of ΔP_0 is equal to zero because the meniscus is flat far from the faces. The shape of the meniscus is given by eq 8.

$$h(x) = t\left(\frac{\exp(-x/x_C) + \exp(x/x_C)}{\exp(-r/x_C) + \exp(r/x_C)}\right) \qquad (8)$$

Equation 8 can be used to find the contributions to the change in capillary, E_C (J), and gravitational, E_G (J), energies when two objects approach one another. The change in capillary energy is found from the change in the surface area at the interface when two objects move relative to one another. We define $\Delta\lambda$ as the difference in the arc length defined by $h(x)$ for two faces separated by $2r$ (plus a flat piece of the PFD/H$_2$O interface to keep the two lengths comparable) and two faces separated by infinity. The change in capillary energy is found by multiplying $\Delta\lambda$ by the width, w (m), of the faces and the interfacial free energy. To find a solution for the change in capillary energy when two objects with positive menisci come into contact, we assume that the heights of the objects are the same and that the widths are five times their heights: $E_C = 5\Delta\lambda t\gamma$. We ignore the menisci that extend beyond the perpendicular to the edges of the faces. The area at the interface decreases as the faces approach one another; the capillary energy therefore decreases, and the objects are drawn toward one another. The change in gravitational energy is found from lowering the PFD in the positive menisci to the level of the PFD/H$_2$O interface. The change in the sum of the capillary and gravitational energies, ΔW (J), relative to an infinite separation is given in Figure 21 for objects with heights and widths of 1 × 5 mm, 100 × 500 μm, and 10 × 50 μm.

Figure 21 indicates that the energy of interaction increases by 3 orders of magnitude when the height and width both increase by 1 order of magnitude. Because the energy of interaction scales as the width of the face (see above), the energy of interaction scales as the square of the height of the objects. This point is important for two reasons. (i) The curves for the

(65) Bowden, N.; Grzybowski, B.; Whitesides, G. M., unpublished results.
(66) Paunov, V. N.; Kralchevsky, P. A.; Denkov, N. D.; Nagayama, K. *J. Colloid Interface Sci.* **1993**, *157*, 100−112.
(67) Chan, D. Y. C.; Henry, J. D., Jr.; White, L. R. *J. Colloid Interface Sci.* **1981**, *79*, 410−418.
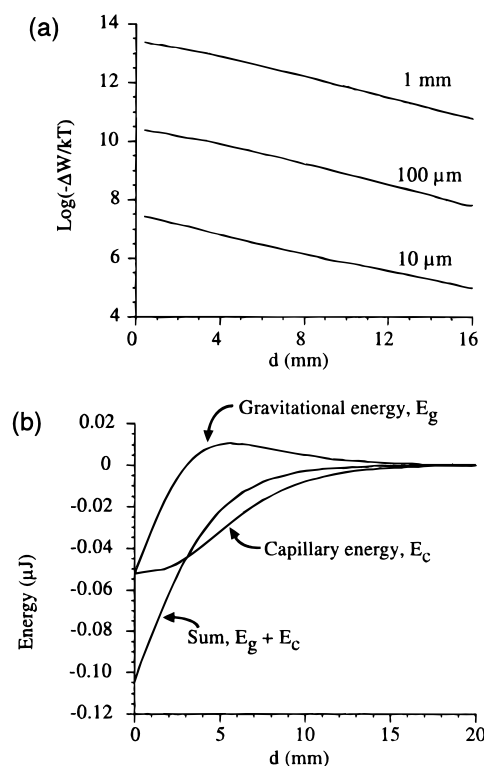
Figure 21. (a) Change in energy as two objects with dimensions (height × width) along the face of 1.0 × 5.0 mm, 100 × 500 μm, and 10 × 50 μm are brought from infinity to a separation, d, is plotted. (b) Change in capillary, gravitational, and total energy as objects of height 1 mm and width 5 mm are brought from infinity to a separation, d.

energy of interaction for the various heights are parallel to one another and are well understood. (ii) We can estimate how the changes in dimensions of the objects will affect their energy of interaction without additional calculations based on the Laplace equation. We apply this knowledge to the problem of finding how far the hexagons are pulled into the interface.

The contributions of the capillary and gravitational energies to the total energy as a function of separation for two faces 1.0 mm high by 5.0 mm wide are shown in Figure 21. The total energy of interaction and the capillary energy are always decreasing with decreasing separation between the faces, although the contribution from the gravitational energy is positive at a separation around 5 mm. The gravitational and capillary energy of interaction both scale with the square of the heights of the objects.

We solved the equations for the idealized cases of an isolated, infinitely long face or two infinitely long faces interacting through capillarity. Although we assumed the faces had positive menisci, these equations describe positive and negative menisci equally well. The capillary and gravitational energies shown in Figure 21 are the same for positive or negative menisci.

We can estimate how far hexagons with a centrosymmetric pattern of hydrophobic faces are pulled into the PFD/H$_2$O interface from the graph in Figure 21a. There are three forces acting on the hexagons: capillary, gravitational, and buoyant forces. The capillary forces result from changes in the area at the PFD/H$_2$O interface; the gravitational forces result from the lowering of the PFD in the menisci to the level of the interface; the buoyant forces result from the hexagons displacing the PFD as they are pulled into the interface. The capillary and gravitational forces either raise or lower the hexagons relative to the interface. For faces with positive menisci, the capillary and gravitational forces pull the hexagons into the interface;

Table 4. Aggregates Formed by the Hexagons. Number of Hydrophobic Faces Increases Going Down the List

Centrosymmetric (in-plane)		Noncentrosymmetric (tilted)	
Hexagon	Structure	Hexagon	Structure
⬡	ordered: close-packed hexagonal lattice		
		⬡	ordered: dimers
⬡	ordered: lines	⬡	ordered: trimers
		⬡	partly disordred: lines
⬡	ordered: open hexagonal lattice	⬡	partly ordered: cyclic hexamers, others
		⬡ ⬡	partly ordered: chiral lines
⬡	ordered: open hexagonal lattice	⬡	partly ordered: dimers, tetramers
		⬡	ordered: lines
		⬡	disordered
⬡	ordered: close-packed hexagonal lattice		

for faces with negative menisci, the capillary and gravitational forces push the hexagons out of the interface. The buoyant forces oppose the capillary and gravitational forces. The buoyant forces arise because the hexagons ($\rho = 1.05$ g/cm^3) floating at the PFD ($\rho = 1.91$ g/cm^3)/H$_2$O ($\rho = 1.00$ g/cm^3) interface displace the PFD as they are pulled into the interface. The buoyant forces are also gravitational forces, but there is an important distinction between "gravitational" and "buoyant" forces. The gravitational forces result from changes in the heights of the PFD and water in the menisci; the buoyant forces result from changes in the heights of the PFD and water due to the displacement of the liquids by the hexagons as they move up and down relative to the interface.

A complete derivation is given in the Supporting Information. Table 2 gives the depths to which we estimate the centrosymmetric hexagons sink into the interface. These values agree qualitatively with those we observe, although we have not quantified these observations.

Conclusions

Capillary Interactions Provide a Method of Forming Ordered Aggregates of mm-Sized Objects. A common type of structural element—hexagonal plates with hydrophilic tops, hydrophobic bottoms, and different combinations of hydrophilic and hydrophobic edge faces—self-assembles into aggregates having a range of structures (Table 4). In each case, the hexagons assembled in a way that matched the contours of the menisci on opposing faces or vertexes of adjacent hexagons. Most of these arrays assembled with face-to-face contact involving hydrophobic faces with large, positive menisci. A few assembled through vertex-to-vertex contacts, but these also involved recognizable interactions between menisci. The tilt of the hexagons at the interface controlled the height of the positive

menisci along the hydrophobic faces and strongly influenced (in some instances, determined) the aggregates into which the hexagons assembled.

The process in which these ordered aggregates formed had four characteristics: (i) In most instances, aggregation was partially or completely reversible. Some aggregates (e.g., [1] and [1,4] hexagons) associated and dissociated freely under conditions of strong agitation. Other aggregates (e.g., those from [1,2] and [1,2,3,4] hexagons) formed some structures joined through mismatched menisci that were unstable to strong agitation, but other aggregates formed structures joined with matched menisci that were stable. (ii) The arrays formed rapidly (usually less than 30 min). The capillary forces were attractive (or repulsive) over distances comparable to several times the heights of the faces of the hexagons. (iii) There were three important capillary interactions: positive menisci attracted one another, negative menisci attracted one another, and positive and negative menisci repelled one another. The relative importance of positive and negative menisci depended on the position of the hexagons relative to the mean plane of the interface: PDMS hexagons with a few hydrophobic faces interacted predominantly through the menisci at these faces, and hexagons with high density ($\rho_{PDMS} > 1.05$ g/cm^3) and those with many hydrophobic faces were buried further in the interface and showed larger negative menisci and stronger interactions involving these menisci. (iv) Even when at closest approach, the hexagons could move laterally relative to one another because they were separated by a thin layer of PFD. This lateral movement allowed misalignments in the initial assembly of two hexagons to correct themselves.

In two instances (those involving [1,2] and [1,2,3,4] hexagons, Figures 10 and 15), we observed the formation of ordered aggregates in a hierarchical process: the hexagons first assembled into small arrays on the basis of strong interactions between some or all of their hydrophobic faces; these arrays subsequently assembled into larger, ordered aggregates on the basis of weak interactions between the hydrophilic faces and any exposed hydrophobic faces (the exposed hydrophobic faces were buried in the PFD/H$_2$O interface due to the tilt of the hexagons and did not assemble into contact when agitated strongly). In addition, in many systems, the weak, negative or positive menisci pulled the initially formed aggregates into loose, semi-ordered aggregates if agitation was weak or absent.

These Systems are Characterized by Meso-Scale Interactions. A mesoscopic system is one where the characteristic length of the phenomenon is on the same order of magnitude as the size of the objects. In these experiments we have characterized the self-assembly of hexagons ($\sim$1 mm thick and $\sim$5 mm in diameter) by lateral capillary forces. The menisci are $\sim$1 mm tall and decay exponentially with a decay length of approximately 1.2 mm. The hexagons and the menisci have about the same size; thus, it is a mesoscopic system.

Because this system is mesoscopic, we see three phenomena. (i) Hexagons with an unsymmetric pattern of hydrophobic faces are tilted at the interface. (ii) The assembly is reversible at high rates of agitation. (iii) Hexagons interact with one another by faces that are not in contact. In some instances we infer a short separation between two faces (such as between [1] hexagons in a dimer), and in other instances we can see a short separation between two faces although their vertexes may be in contact (such as in the vertex-to-vertex assembly). These phenomena would not be seen if the range of the interaction between the faces were much smaller or larger than the dimensions of the objects.

Directional Capillary Interactions Can Be Considered as a Kind of Bond. The "Capillary Bond". We suggest that the capillary interactions between these functionalized plates can be viewed as "bonds", analogous in important ways to the chemical bonds between atoms. Both types of bonds have characteristic energies and directionality, and both can, in principle, be described by well-defined potential functions. Both also have important characteristics related to their signs and symmetries. For atoms in molecules, the signs and amplitudes of orbitals determine their ability to overlap constructively; for capillary aggregates, the sign of the meniscus (relative to the mean plane of the interface) and its amplitude determine its contour and thus the strength of its interaction with another meniscus.

In this model, the hexagons are analogous to the atoms in molecules, or to the molecules in noncovalent aggregates, and the capillary bonds are the interactions holding them together. Capillary and chemical bonds differ, of course, in the very important sense that the former can be described classically and the latter require quantum mechanics.

We can tailor the strength of the capillary bond by any strategy that changes the shape of the interacting menisci: that is, by changing the width of the faces, the pattern of hydrophobic and hydrophilic regions on a hexagon or on an face of a hexagon, the tilt of the hexagon, the shape of the interacting interfaces, the density of the hexagon relative to the fluid phases, and the interfacial free energies of the five types of interfaces (γ_{PFD/H_2O}, γ_{PDMS/H_2O}, $\gamma_{PDMS/PFD}$, $\gamma_{oxidized\ PDMS/H_2O}$, and $\gamma_{oxidized\ PDMS/PFD}$).

The Capillary Bond Matches the Shapes of Menisci. Capillary and chemical bonds form such that the overlapping menisci are matched in symmetry and amplitude; analogous statements describe the overlap of orbitals in chemical bonds. In aggregates held together by capillary bonds, the hexagons assemble to match the contours of the menisci on the opposing faces. The shape of the menisci is determined by the system (shape of the objects, pattern of hydrophobic faces, and densities of the liquids and PDMS), and it is different for each set of hexagons. This flexibility in defining the shapes of the menisci makes this system an exceptionally flexible one with which to study the chemistry and physics of mesoscale self-assembly.

Comparisons and Contrasts Between Mesoscale Self-Assembly and Noncovalent, Molecular-Scale Self-Assembly. MESA and molecular self-assembly operate at vastly different regions of size and time, but MESA, nonetheless, has several similarities to molecular-scale self-assembly. (i) The shape and patterns of functional groups (H-bond donors and acceptors, hydrophobic groups and charged groups for molecular self-assembly, and hydrophobic faces for this system of MESA) on the molecules and objects are important in determining the arrays that form. (ii) The directionality of the chemical and capillary bonds define and predict the structure of the final arrays. (iii) Attractive forces due to capillarity are comparable in strength to the disruptive forces due to shear during agitation.

Important differences between mesoscopic self-assembly and molecular self-assembly limit any direct comparison between these two types of processes. One difference is the kinetics of formation of the arrays. MESA has much slower rates of encounter and of collision within an encounter complex than do molecules: these numbers for MESA are, respectively, ~1 s⁻¹ for collision (at a surface density of 3800 hexagons m⁻² and agitation of $\omega = 1.5$ s⁻¹) and an undefined frequency for subsequent vibrations within the encounter complex; for a bimolecular reaction (at 10^{-3} M⁻¹ and 298 K), collisions occur at ~10^4 sec⁻¹, and vibrations within the encounter complex occur at ~10^{12} sec⁻¹.[68] The interactions between particles in MESA are classical; the interactions between molecules are quantum mechanical. Only a small number of interacting objects are present in MESA (typically ~10^2); the number of molecules interacting is typically > 10^{15} in molecular self-assembly. MESA is a nonthermal system: the distribution of kinetic energies is heterogeneous across the surface of the fluids as it swirls and is not described by the Boltzmann equation and standard thermodynamics. The behavior of molecules is well described by classical thermodynamics and statistical mechanics.

Impact. We believe that MESA will find applications in a broad range of areas from microelectronics and photonics to microelectromechanical systems (MEMS). This type of self-assembly has direct potential for applications in the precision assembly of small objects because self-assembly is inherently error-correcting. Although this work dealt with two-dimensional self-assembly, related work has extended the idea of MESA to three dimensions.[8-10,69] This extension to three dimensions is significant because most methods of fabrication on the submillimeter scale are inherently two-dimensional.

MESA also has potential applications in chemistry. MESA can provide models of chemical systems or abstract lattice models in chemical theory. MESA can stimulate new ways to assemble objects; assembly through lateral capillary forces is just one method. MESA could be used to study the interactions between surfaces. Finally, MESA can be a model for self-assembly at the molecular scale that may stimulate ideas and strategies, even if it is an imperfect model in many respects.

We believe that observations made with mm-scale objects are relevant to interactions of μm-scale objects. The scaling of the important parameters describing the forces is linear: the buoyant forces, mass, and free energies of interaction all fall off as the reciprocal of the cube root of the length of the objects (assuming them to be cubes). Although this study dealt with mm-scale objects, the ideas and forces should scale to μm-scale objects;[7] the μm range of sizes is a particularly interesting and important region for electronics, MEMS, and sensors.

Experimental Section

General. PDMS (Sylgard 184), a product of Dow Corning, was purchased from Brownell Electronics, Inc. (Woburn, MA). PDMS was made by mixing the two components (10:1 by weight), degassing under vacuum, and curing in a 60 °C oven for no less than 3 h. Perfluorodecalin, perfluoromethyldecalin, crystal violet, and Sudan red 7B were purchased from Aldrich and used as received. Hexagonal brass rods were purchased from Small Parts, Inc. (Miami Lakes, FL) and cleaned with water, hexane, and methylene chloride before use. The gold (50-nm thick) coated glass slides used to determine the tilt angles of the hexagons were prepared using procedures described previously.[70,71] The plasma cleaner was a Harrick model PDC-23G and attached to a standard vacuum pump. All of the oxidations were done under continuous vacuum (~200 milliTorr) and on the medium setting on the plasma cleaner.

(68) Atkins, P. W. *Physical Chemistry*; 4th ed.; W. H. Freeman and Company: New York, 1990.

(69) Tien, J.; Breen, T. L.; Whitesides, G. M. *J. Am. Chem. Soc.* **1998**, *120*, 12670−12671.

(70) Wilbur, J. L.; Kumar, A.; Kim, E.; Whitesides, G. *Advanced Materials* **1994**, *6*, 600−604.

(71) Xia, Y.; Whitesides, G. M. *Angew. Chem., Int. Ed.* **1998**, *37*, 7, 550−575.

Self-assembly of [1,2,3,4] hexagons. We describe the self-assembly of the [1,2,3,4] hexagons. The process that we followed to characterize the arrays that self-assembled from the [1,2,3,4] hexagons was representative of the process that occurred for all of the hexagons. The description of the process can be found in the Supporting Information.

Supporting Information Available: Complete derivation of the estimate for the distance the hexagons are pulled into the interface, fabrication of the hexagons, visualizing the menisci, and self-assembly of [1,2,3,4] hexagons (PDF). This material is available free of charge via the Internet at http://pubs.acs.org.

JA983882Z